iScience

CellPress
OPEN ACCESS

Article

Lactylome analysis reveals potential target modified proteins in the retina of form-deprivation myopia

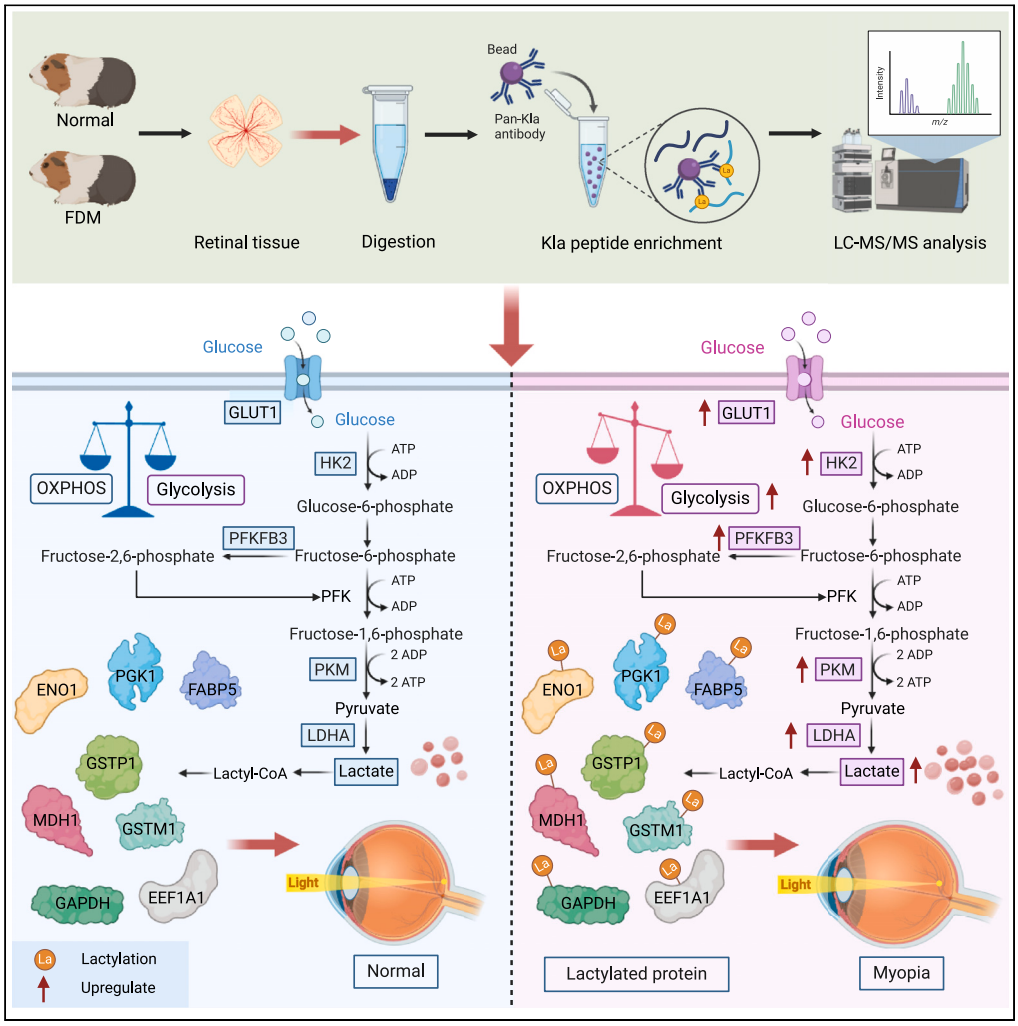

Jiaojiao Feng, Xiaoniao Chen, Runkuan Li, ..., Yifan Song, Jike Song, Hongsheng Bi

edusjk@163.com (J.S.)
hongshengbi1@163.com (H.B.)

Highlights

Increased glycolytic flux and lactate accumulation in the FDM retina

The first protein lysine lactylome in the myopic retina

Lactylated proteins were significantly enriched in cellular metabolic processes

Lactylome in experimental myopic retinas reveals potential target biomarkers

Feng et al., iScience 27, 110606
September 20, 2024
https://doi.org/10.1016/j.isci.2024.110606

iScience

CellPress
OPEN ACCESS

Article

Lactylome analysis reveals potential target modified proteins in the retina of form-deprivation myopia

Jiaojiao Feng,[1,5] Xiaoniao Chen,[4,5] Runkuan Li,[1,5] Yunxiao Xie,[2,3] Xiuyan Zhang,[2,3] Xiaoxiao Guo,[1] Lianghui Zhao,[1] Zhe Xu,[1] Yifan Song,[1] Jike Song,[1,3,*] and Hongsheng Bi[2,3,6,*]

SUMMARY

The biological mechanisms underlying the development of myopia have not yet been completely elucidated. The retina is critical for visual signal processing, which primarily utilizes aerobic glycolysis to produce lactate as a metabolic end product. Lactate facilitates lysine lactylation (Kla), a posttranslational modification essential for transcriptional regulation. This study found increased glycolytic flux and lactate accumulation in the retinas of form-deprived myopic guinea pigs. Subsequently, a comprehensive analysis of Kla levels in retinal proteins revealed that Kla was upregulated at 124 sites in 92 proteins and downregulated at three sites in three proteins. Functional enrichment and protein interaction analyses showed significant enrichment in pathways related to energy metabolism, including glutathione metabolism, glycolysis, and the hypoxia-inducible factor-1 signaling pathway. Parallel-reaction monitoring confirmed data reliability. These findings suggest a connection between myopia and retinal energy metabolism imbalance, providing new insights into the pathogenesis of myopia.

INTRODUCTION

Myopia is a highly prevalent ocular disorder worldwide, with prevalence rates as high as 10–30% in adults in many countries. In some regions of East and Southeast Asia, the prevalence among young adults can reach as high as 80–90%.[1,2] It is characterized by an excessively elongated axial direction of the eye that causes the image to focus before the retina.[3] When abnormal visual signals occur, the retina produces regulatory signaling molecules (such as dopamine,[4] retinoic acid,[5] and nitric oxide[6]) that are delivered to the choroid and trigger a reaction in the sclera, leading to the abnormal metabolic process of scleral remodeling. Although the retina plays a vital role as a signal source in visually driven eye growth, the biological mechanisms underlying the rapid elongation of the eye's axial length (AL) in response to blurred retinal imaging remain poorly understood.[7]

Posttranslational modifications (PTMs) of proteins, such as phosphorylation,[8] acetylation,[9] glycosylation,[10] ubiquitination,[11] S-nitrosylation,[12] and methylation,[13] are critical mechanisms that regulate protein function. They play vital roles in modulating various physiological and pathological processes within cells. Previous studies have shown that PTMs play an irreplaceable role in the pathogenesis of myopia.[12,14–16] Elevated levels of phosphorylation of retinal connexin 36 in form-deprived myopic mice have been linked to an increase in functional gap junction coupling in amacrine cells that actively adapt to the defocused state in the myopic retina.[14] However, altered levels of c-Jun N-terminal kinase-1 phosphorylation modulated aquaporin-1 and choroidal thickness during recovery from form deprivation myopia (FDM).[15] Another study found that the inflammatory response in the myopic retina could be inhibited by decreasing the phosphorylation level of protein kinase B (AKT) and the expression of nuclear factor κ-light chain-activated B enhancer.[16] Significantly reduced levels of S-nitrosylation of α-enolase in the retina of myopic mice were thought to possibly play a key role in the pathogenesis of myopia.[12] However, few studies have focused on PTMs, and the role of most PTMs in myopia has not yet been elucidated.

Mammalian retinas exhibit a preference for converting glucose into lactate, rather than completely metabolizing it to carbon dioxide through oxidative phosphorylation, even in the presence of sufficient oxygen. This metabolic phenomenon, known as aerobic glycolysis or the Warburg effect,[17,18] resembles the metabolic behavior observed in cancer cells. The retina, a highly energy-demanding tissue, requires substantial amounts of energy to sustain neuronal activity for processes, such as phototransduction and neurotransmission.[19] Thus, aerobic

[1]Shandong University of Traditional Chinese Medicine, Jinan 250014, China
[2]Affiliated Eye Hospital of Shandong University of Traditional Chinese Medicine, Jinan 250002, China
[3]Shandong Academy of Eye Disease Prevention and Therapy, Shandong Provincial Key Laboratory of Integrated Traditional Chinese and Western Medicine for Prevention and Therapy of Ocular Diseases, Jinan 250002, China
[4]Department of Ophthalmology, Chinese PLA General Hospital, Beijing 100853, China
[5]These authors contributed equally
[6]Lead contact
*Correspondence: edusjk@163.com (J.S.), hongshengbi1@163.com (H.B.)
https://doi.org/10.1016/j.isci.2024.110606

glycolysis occurs at a high frequency in both intact and isolated retinal cells,[20] with 80–96% of glucose converted to lactate.[21] A study published in Nature in 2019 by Prof. Yingming Zhao found that lactate accumulated during metabolism could act as a precursor to modify lysine residues in proteins, a process called lysine lactylation (Kla).[22] Kla catalyzes the lactyl group derived from L-lactate to combine with lysine in a reversible covalent manner via the enzymatic reaction of p300.[22,23] Numerous studies have emphasized the role of Kla in regulating various cellular processes, particularly tumor energy metabolism, mitochondrial dysfunction, and diseases induced by hypoxia.[24–26] Hypoxia led to increased levels of Yin Yang-1 lactylation in retinal microglia, which transcriptionally activated fibroblast growth factor 2 expression, thereby promoting angiogenesis.[27] Given the reliance of the retina on aerobic glycolysis to produce lactate, it is evident that Kla may play a pivotal role in retinal tissue homeostasis and function.

The FDM model is one of the primary animal models used for myopia research.[28] Although the transcriptional regulatory mechanisms of several myopia-related genes in FDM animal models have been investigated,[4–6] limited studies on protein modifications have hindered a comprehensive understanding of the molecular basis underlying the pathogenesis of myopia. In this study, we performed the first proteome-wide Kla modification analysis of the myopic retina, revealing the distribution pattern of Kla in the experimental myopic retina and providing a new understanding of the retinal regulatory mechanism of myopia at the levels of PTMs.

RESULTS

Form-deprivation myopia

Before the form-deprivation treatment, there was no statistical difference in AL or refraction for all eyes in each group ($p > 0.05$) (Figures 1A and 1B). However, following two weeks of form-deprivation treatment, the mean sphere refraction of eyes in the FDM group (-2.38 ± 1.01 D, $n = 30$) was significantly more myopic than that of eyes in the NC group ($+0.75 \pm 1.13$ D, $n = 30$, $p < 0.01$) (Figure 1A). Additionally, the AL of eyes in the FDM group (8.24 ± 0.11 mm, $n = 30$) was significantly longer than that of eyes in the NC group (8.05 ± 0.07 mm, $n = 30$, $p < 0.01$) (Figure 1B). These results confirmed the successful establishment of the FDM in the animal models. Therefore, retinas from both the FDM and NC groups were considered for this study (Figure 1C).

Enhanced glycolytic metabolic flux contributes to lactate accumulation

To investigate glycolytic metabolic fluxes in the retinas, we assayed the levels of key rate-limiting enzymes involved in glycolysis. These enzymes included glucose transporter 1 (GLUT 1), hexokinase 2 (HK 2), 6-phosphofructo-2-kinase/fructose-2,6-biphosphatase 3 (PFKFB 3), pyruvate kinase M (PKM), and lactate dehydrogenase A (LDHA) (Figure 2A). Comparing the retinas of the NC group to those in the FDM group, we observed an overall significant upregulation in the expression of these proteins (Figure 2B). Since LDH is critical in catalyzing the final step of aerobic glycolysis, we further assessed changes in LDH activity. We found that LDH activity was significantly higher in the retina of the FDM group (1612.4 ± 49.84 U/g) than that of the NC group (1415.37 ± 125.9 U/g, $p < 0.05$) (Figure 2C). It was demonstrated that the lactate content in the FDM group (34.61 ± 9.26 μmol/g) was significantly higher than that in the retina of the NC group (21.12 ± 1.94 μmol/g, $p < 0.01$) (Figure 2D). These results suggest that there is a significant increase in glycolytic metabolic flux and, thus, lactate accumulation in the retinas of eyes in the FDM group.

Lysine lactylation abundantly expressed in the retina

To determine whether changes in lactate content in the guinea pig retina led to alterations in protein lactylation modifications, we conducted western blotting of lactylated proteins in the retina using a pan-antibody specific for lysine lactylation (Pan-Kla). The loading control by Coomassie blue staining was used to ensure that equal amounts of protein were loaded in each lane. As shown in Figure 3A, lactylation modifications were widely present in the retinas of guinea pigs, and form deprivation treatment significantly altered the levels of protein lactylation modifications in guinea pig retinas. Western blotting results indicated that, at the histone level, the level of lactylation was significantly decreased in the FDM group, whereas at the non-histone level, the level of lactylation was markedly enhanced in the FDM group. To further validate our findings, we performed immunofluorescence of the retina using Pan-Kla, and the relative quantitative analysis confirmed a significantly enhanced level of lactylation modification in the retinas of the FDM group ($p < 0.05$) (Figure 3B). Additionally, the proteins with increased lactylation levels were mainly distributed in the inner nuclear layer and outer nuclear layer of the retina (Figure 3C). These results indicate significantly elevated levels of lactylation modifications in the retinas of guinea pigs with FDM.

Lactylome analysis

Differential lactylated proteins analysis

To comprehensively investigate changes in Kla protein in the retina, quantitative lactylome profiling was performed following the flowchart shown in Figure 3D. To verify the reliability of the mass spectrometry data, we examined the length distribution of the characterized peptides. As shown in Figure S1, the majority of lactylated peptides ranged from 7 to 20 amino acids in length, as expected for tryptic peptides. In the label-free quantitative proteomic analysis, 1,989 lactylation sites on 848 proteins were characterized, of which 1,500 sites on 691 proteins could be quantified (Table S1). After normalization of the total quantitative proteins, it was demonstrated that the level of lactylation increased at 124 sites on 92 proteins and decreased at three sites on three proteins in the retinas of the FDM group compared to that in the NC group (Figure 3E and Table S2). Furthermore, nine core histone Kla sites were identified (Table S3). Of the identified 94 lactylated proteins, 79.8% contained one lactylated site, 11.7% contained two lactylated sites, 3.2% contained three lactylated sites, 4.3% contained four lactylated sites,

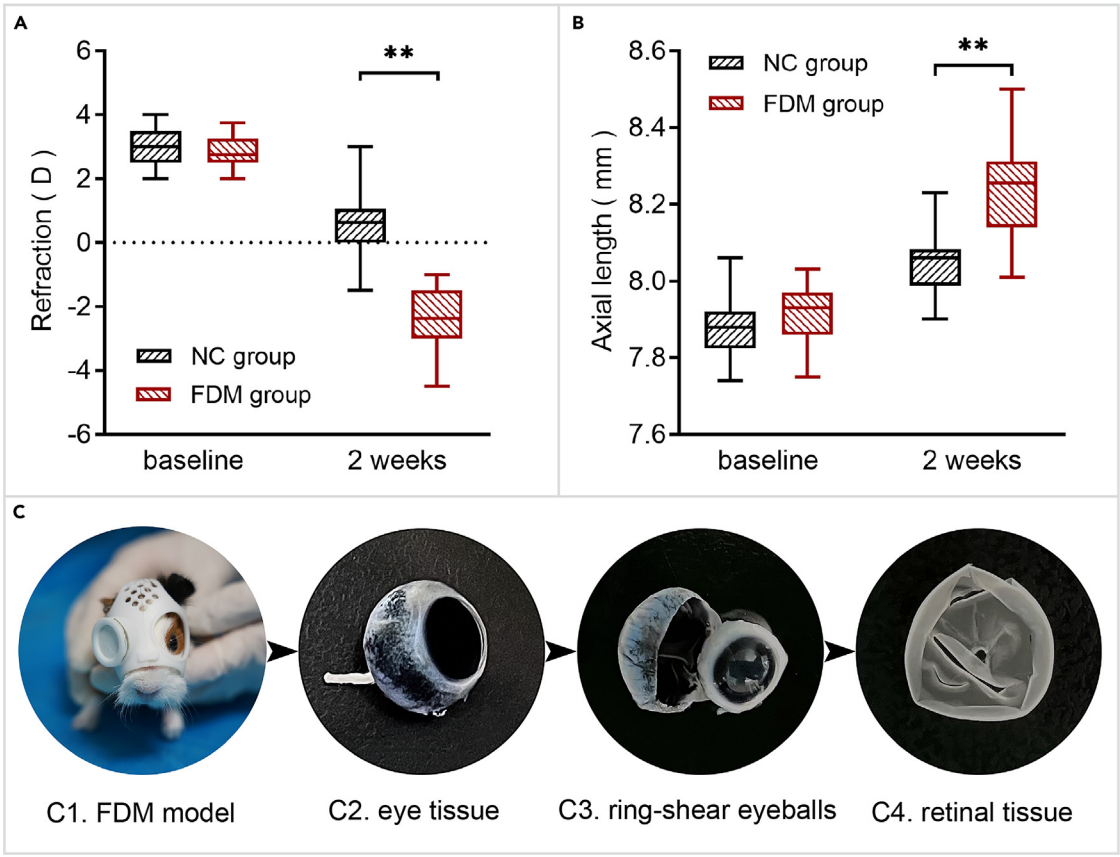

Figure 1. Changes in ocular biological parameters

Refraction (A) and axial length (B) at the beginning and end of treatment in the NC group and FDM group.

(C) Schematic diagram of retinal tissue sampling. FDM group, form-deprivation myopia group; NC group, normal control group; $^{**}p < 0.01$.

and 1.1% contained five lactylated sites (Figure 3F). Among them, SUGP2 contained five significantly altered lactylated sites, whereas CTTN, SAG, MECP2, and THRAP3 contained four lactylated sites. Furthermore, we quantified changes in the levels of protein lactylation in each group, and the results are shown in Figure 3G. Compared with that of the NC group, the FDM group showed that the proteins with the most significant upregulation of Kla levels included FABP5_K61, PGD_K38, A0A286XP64_K155, HMGB1_K12, and HNRNPL_K62, while the most significant downregulation of Kla levels included SYN1_K618, SF3A2_K10, and PGAM1_K113.

Motif analysis of lactylation sites

To investigate the sequence patterns surrounding the lactylation sites, we used motif analysis to analyze the ten amino acids flanking the identified lactylation sites. The results showed that a total of six definitively conserved motifs were identified, namely, Kla_xxxxxxxK, Kla_xG, Kxxxxxxx_Kla, Kxxxxxxxx_Kla, Kxxxxxx_Kla, Kla_SxxxxxxxxK (Figure 4A). We generated a heatmap of the amino acid sequences around the lactylation site to further analyze these patterns. The heatmap shows the enrichment or deletion of amino acids upstream and downstream of all the identified lactylation sites (Figure 4B). Alanine (A) and lysine (K) were found to be often abundant near Kla sites. Conversely, cysteine (C) and leucine (L) were often reduced around the Kla site. Notably, glycine (G) and proline (P) were remarkably abundant at sites −1 to −5 or +2 and +3, whereas they were decreased at other sites. These results reflect different preferences for amino acids around the Kla site.

Subcellular localization analysis

To better characterize the lactylated proteins in the FDM and NC groups, we analyzed the subcellular localization of the lactylated substrates. Most lactylated proteins were localized in the nucleus (41.05%), whereas 36.84% and 8.42% were distributed in the cytoplasm and mitochondria, respectively, and 8.42% were capable of cytoplasmic-nuclear shuttling, indicating that lactylated proteins have a diverse cellular distribution (Figure 5A). In addition, we characterized the subcellular localization of the differentially lactylated proteins (DLPs) using network analysis. A total of 38 proteins had increased levels of lactylation in the nucleus, 34 proteins had increased levels of lactylation in the cytoplasm, and eight proteins with increased levels of lactylation were found in the mitochondria (Figure 5B).

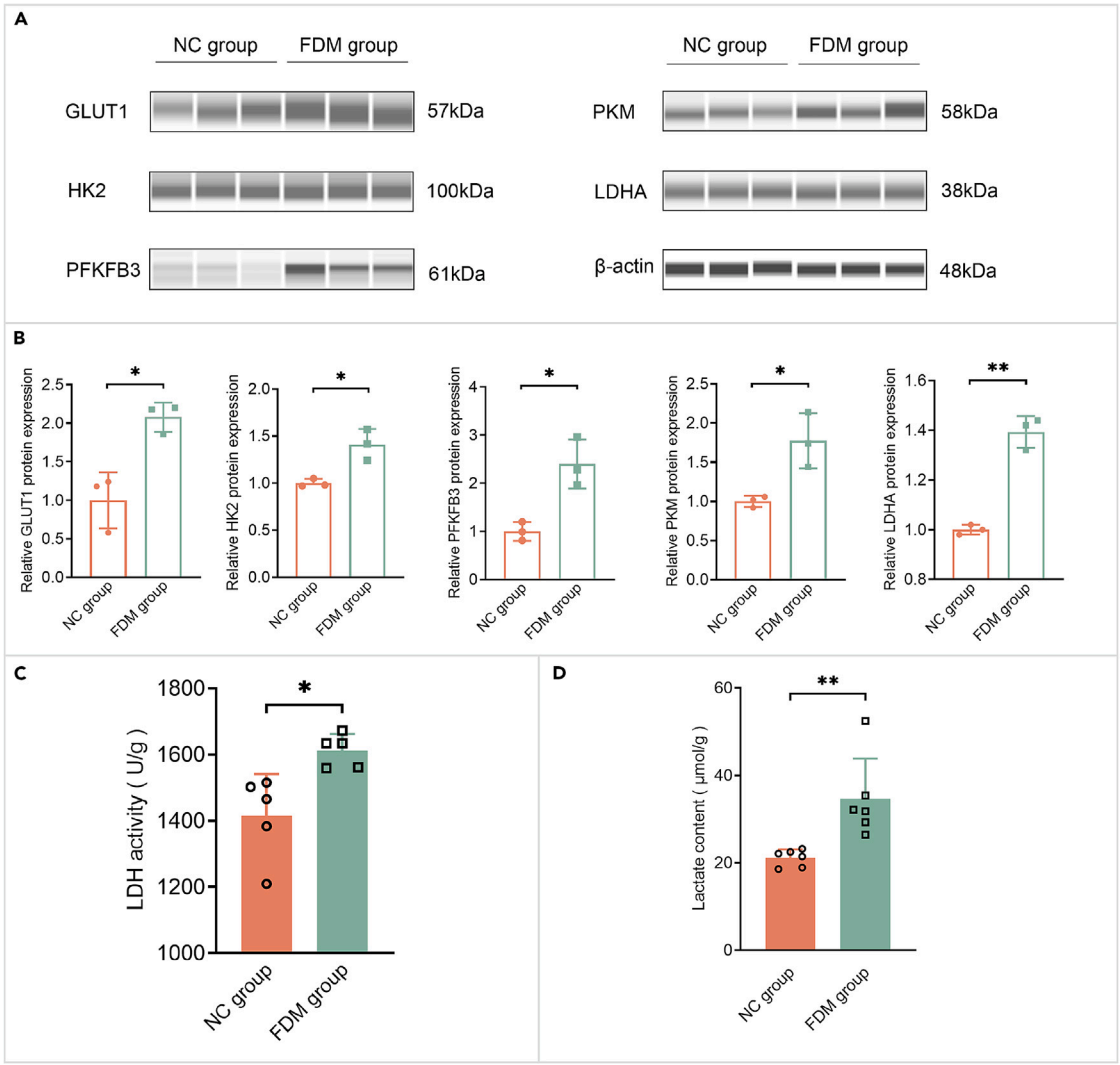

Figure 2. Retinal glycolytic metabolism and lactate changes

(A) Protein expression levels of GLUT1, PFKFB3, PKM2, and LDHA in the NC group and FDM group were detected by the digital capillary western blotting. β-actin served as a loading control.

(B) Quantification of proteins was normalized to the relative value of β-actin expressed as mean ± SD, $n = 3$ per group.

(C) Assay of LDH activity in both groups, $n = 5$ per group.

(D) Lactate content after treatment for 2 weeks, $n = 6$ per group. *$p < 0.05$, **$p < 0.01$.

Functional annotation and enrichment analysis

We conducted a gene ontology (GO) functional enrichment analysis of the DLPs. Biological process enrichment analysis showed that most DLPs were involved in various metabolic processes, including the positive regulation of glucose, NADP, gluconeogenesis, and cellular calcium transport (Figure 6A). Additionally, the GO chord plot of DLPs demonstrated that PGD exhibited the most significant enrichment in biological processes, specifically in nicotinamide nucleotide and NADP metabolic processes (Figure 6B). According to cellular component enrichment analysis, DLPs were significantly enriched in the extracellular space, extracellular region, and myelin sheath, with the highest number of proteins found in the extracellular region (Figure 6C). Among the cellular components, fatty acid binding protein 5 (FABP5) was the most enriched and correlated with the cytoplasmic vesicle lumen, secretory granule lumen, extracellular region function, extracellular space, and vesicle lumen (Figure 6D). Molecular functional enrichment analysis revealed that many DLPs were associated with DNA binding, suggesting that lactylated proteins regulate gene expression (Figure 6E). A0A826XP64 had the most abundant molecular functions and was involved in multiple forms of DNA binding (Figure 6F).

Furthermore, pathway analysis using the Kyoto Encyclopedia of Genes and Genomes (KEGG) revealed that DLPs were involved in several signaling pathways associated with the regulation of energy metabolism, including glutathione metabolism, the pentose phosphate pathway,

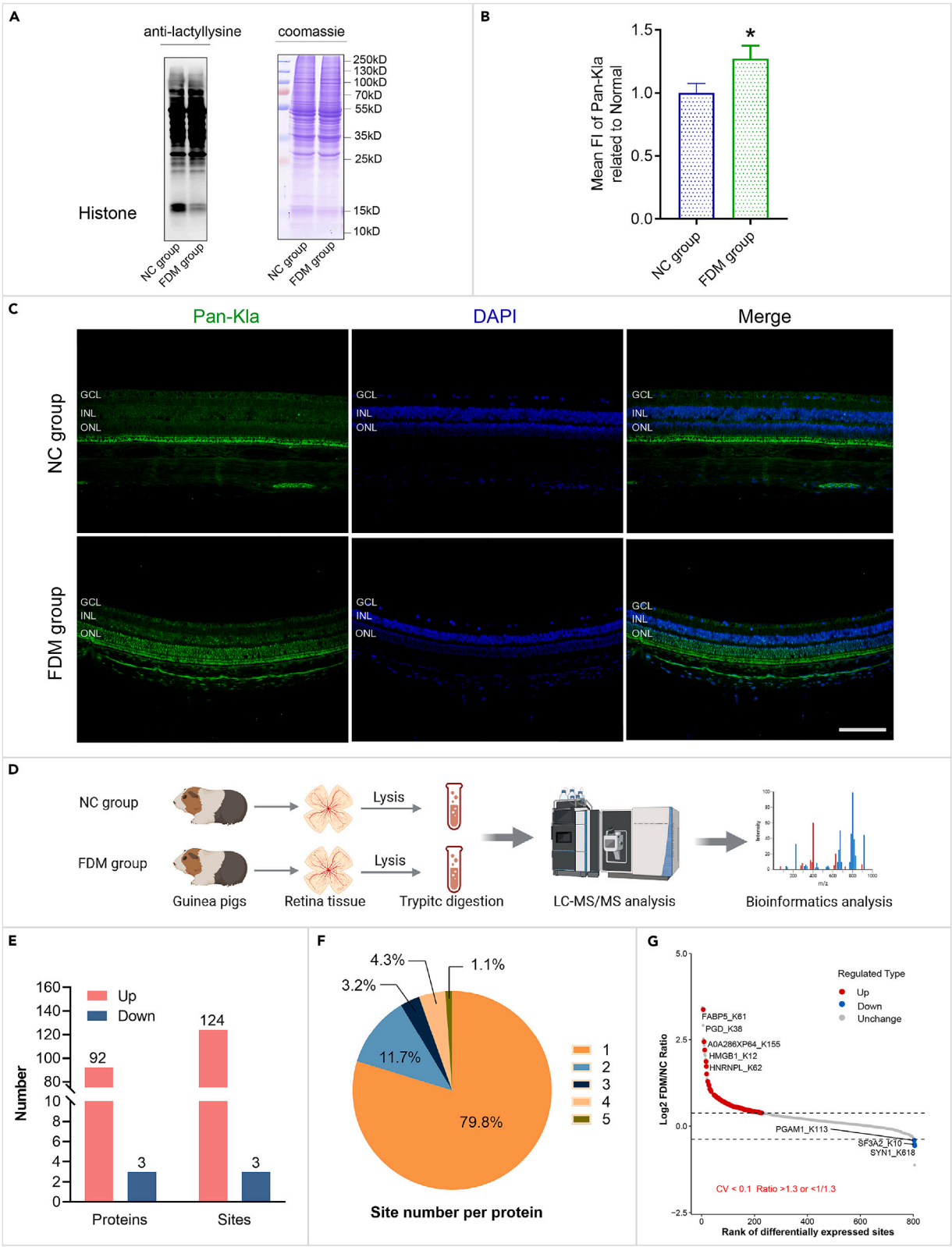
A
anti-lactyllysine
coomassie
250kD
130kD
100kD
70kD
55kD
35kD
25kD
15kD
10kD
Histone
NC group
FDM group
NC group
FDM group
B
Mean FI of Pan-Kla related to Normal
1.5
1.0
0.5
0.0
*
NC group
FDM group
C
Pan-Kla
DAPI
Merge
NC group
FDM group
GCL
INL
ONL
D
NC group
FDM group
Lysis
Lysis
Guinea pigs
Retina tissue
Trypitc digestion
LC-MS/MS analysis
Bioinformatics analysis
E
Number
160
140
120
100
80
10
8
6
4
2
0
Up
Down
92
3
124
3
Proteins
Sites
F
4.3%
1.1%
3.2%
11.7%
79.8%
1
2
3
4
5
Site number per protein
G
Log2 FDM/NC Ratio
5.0
2.5
0.0
−2.5
Regulated Type
Up
Down
Unchange
FABP5_K61
PGD_K38
A0A286XP64_K155
HMGB1_K12
HNRNPL_K62
PGAM1_K113
SF3A2_K10
SYN1_K618
CV < 0.1 Ratio >1.3 or <1/1.3
0
200
400
600
800
Rank of differentially expressed sites

Figure 3. Changes in retinal lactylation and an overview of the lactylome

(A) Western blot analysis of retina by Pan-Kla. Protein molecular weights of 10–15 kDa represent histones and others are non-histone proteins.

(B) Relative quantitative analysis of Pan-Kla fluorescence intensity (FI) in the whole retina. Data are mean ± SD, $n = 3$; *$p < 0.05$.

(C) Immunofluorescence staining showing changes in Pan-Kla in retinal tissue. Scale bar, 100 μm. GCL: ganglion cell layer; INL: inner nuclear layer; ONL: outer nuclear layer.

(D) Diagram of retina tissue collection, lysis, and LC-MS/MS analysis.

(E) Statistical analysis of DLPs and lactylated sites in the FDM group versus the NC group. Red represented upregulated, and blue indicated downregulated.

(F) The number of lactylated sites per lactylated protein.

(G) Scatterplot of DLPs. Downregulated protein is colored blue, while upregulated protein is red. DLPs: differential lactylated proteins.

hypoxia-inducible factor-1 (HIF-1) signaling pathways, and glycolysis/gluconeogenesis (Figure 7A and Table S4). To further analyze the relation between DLPs in the KEGG pathway, we performed a network analysis. Notably, glutathione S-transferase mu 1 (GSTM1) is involved in multiple KEGG pathways associated with drug metabolism-cytochrome P450, metabolism of xenobiotics by cytochrome P450, longevity-regulating pathway-worms, and oxidative phosphorylation. Among the DLPs, PGD was the most significantly upregulated lactylated protein across all KEGG pathways, particularly in the pentose phosphate and oxidative phosphorylation pathways (Figure 7B).

Protein-protein interaction networks

To fully describe protein function, the STRING database was used to analyze the protein-protein interaction (PPI) network of the significantly altered lactylated proteins found in this study to further explore the relation between protein interactions and related biological processes. The lactylated proteins were then assembled using Cytoscape software, and 65 were mapped to the PPI networks (Figure 8). They were categorized into three interrelated clusters: regulation of cellular metabolic processes, nucleic acid metabolic processes, and generation of precursor metabolites and energy. The regulation of cellular metabolic processes was the most obvious cluster of enrichment, suggesting that the proteins involved in this biological process were abundantly modified by Kla. Collectively, these findings suggest that physiological protein interactions between these compounds facilitate functional coordination and cooperation in the retina during FDM development.

Parallel reaction monitoring validation analysis

Parallel reaction monitoring (PRM) is a mass spectrometry-based high-resolution, high-precision targeted proteomics technology that enables targeted relative or absolute quantification of modified peptides through the selective detection of modified peptides. To further validate DLPs in the lactylated proteome, we selected 19 sites of DLPs to perform 4D-PRM validation (Table 1). The targeting validation results of PRM were in high agreement with the results of the non-targeted lactylation proteome, confirming the reliability of the previous data. According to our results, the lactylation of some protein Kla sites in retinas after form deprivation treatment was indeed upregulated, such as FABP5_K61, GSTP1_K111, and VIM_K418, implying that they may serve as targets for myopia therapeutic approaches and merit further investigation.

DISCUSSION

In this study, we made a novel discovery that the protein expression and activity of several key enzymes in the glycolytic metabolic pathway were significantly increased in the retinas of guinea pigs with FDM. This suggests a significant enhancement in glycolytic metabolic flux, which ultimately led to the accumulation of lactate in the retina. The lactate content in the retina was determined to be significantly higher in the FDM group (34.61 ± 9.26 μmol/g) than in the NC group (21.12 ± 1.94 μmol/g). Given the recent discovery that lactate can further mediate the onset of Kla through the generation of lactyl-CoA,[22,23] we examined Kla levels in the retina. It was found that Kla levels were significantly elevated in the FDM retina, with upregulation of Kla levels at 124 sites on 92 proteins and downregulation of Kla levels at three sites on three proteins in the FDM group compared with those in the NC group. Moreover, the DLPs were mainly distributed in the nucleus and cytoplasm. GO and KEGG enrichment analyses, as well as PPI network analyses, revealed that DLPs were mainly involved in cellular metabolism-related biological processes. The reliability of our data were confirmed using PRM analysis, and as the first Kla analysis in myopic retinas, our findings provide a valuable basis for further investigation of Kla function in myopia.

The shift in glucose metabolism from oxidative phosphorylation to aerobic glycolysis generally involves an increase in the expression and activity of glucose transport proteins, glycolytic enzymes, and enzymes that convert pyruvate to lactate.[29] In the present study, the results of retinal capillary western blotting showed that the protein expression levels of GLUT1, HK2, PFKFB3, PKM, and LDHA were significantly upregulated in the retinas of the FDM group compared with those in the NC retina. Further enzyme activity assays revealed that LDH activity was significantly enhanced in FDM retinas. These findings indicate that the glycolytic metabolic flux was significantly enhanced in the FDM retina. The results of the current study further supported previous reports.[30–32] A quantitative proteomics study by Barathi et al. found significant upregulation of LDHA in the retina of experimentally myopic mice, with a trend toward downregulation after atropine treatment.[30] Zhu et al. observed reduced levels of PKM protein expression in the retinas of FDM guinea pigs after atropine treatment.[31] Similarly, in a study by Yu et al., pathway analysis showed significant upregulation of glycolytic enzymes in the retina during the development of experimental myopia in chicks, including PKM2, LDHA, and alpha-enolase.[32] However, in our study, the proteins were detected by western blotting using the corresponding antibodies, whereas previous studies used mass spectrometry to quantify the proteins without further validation of the results. In summary, our findings using different assay techniques consistently demonstrated that the protein expression of key enzymes involved in glycolytic metabolism was significantly enhanced during the development of myopia.

A

Motif Logo	Motif	Motif Score	Foreground Matches	Foreground Size	Background Matches	Background Size	Fold Increase
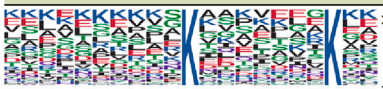	xxxxxxxxxx_K_xxxxxxx Kxx	16.00	274	1989	39305	528826	1.9
	xxxxxxxxxx_K_xGxxxx xxxx	14.21	175	1715	26786	489521	1.9
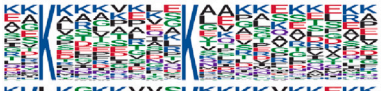	xxKxxxxxxx_K_xxxxxx xxxx	14.48	199	1540	33481	462735	1.8
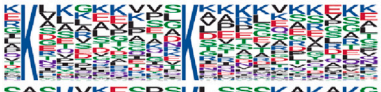	xKxxxxxxxx_K_xxxxxx xxxx	10.28	167	1341	31751	429254	1.7
	xxxKxxxxxx_K_xxxxxx xxxx	8.09	136	1174	27778	397503	1.7
	xxxxxxxxxx_K_Sxxxxxx xxK	13.95	26	1038	1813	369725	5.1

B

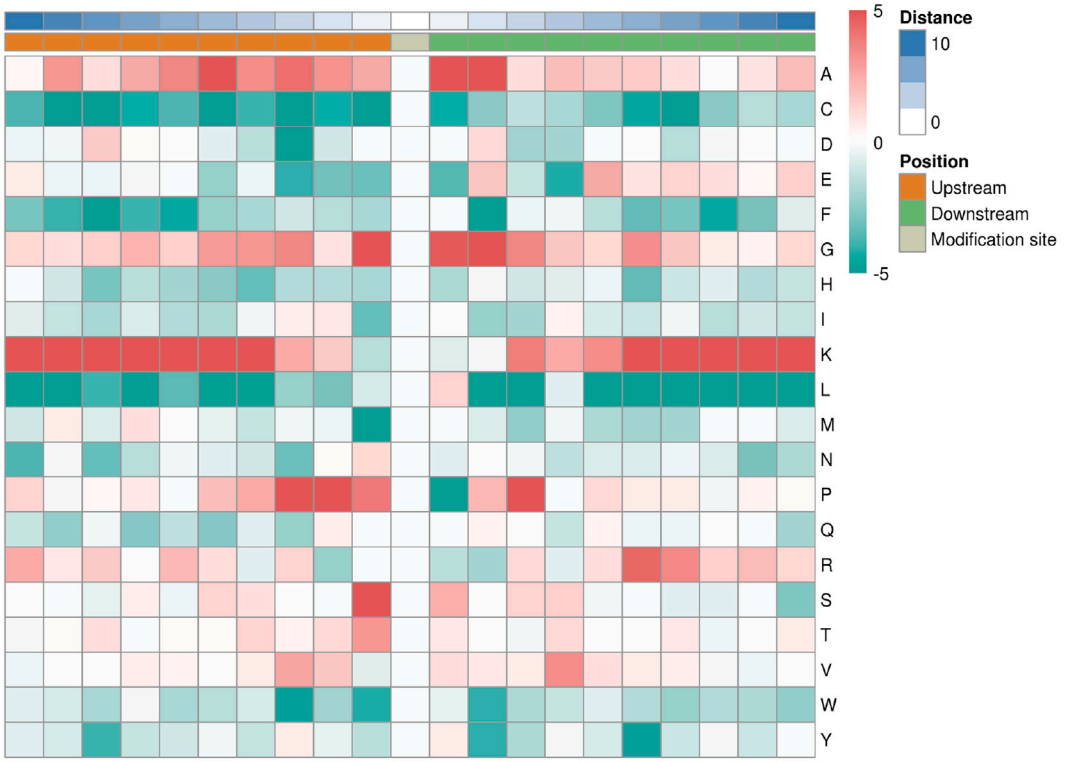

Figure 4. Properties of the Kla peptides in the retina

(A) Lactylation sequence motifs for ±10 amino acids surrounding the Kla sites. Lactylation motifs were constructed with Motif-X software. The central K (at position 0) indicates the lactylation lysine. All the surrounding amino acid residues are indicated with the letters in different heights which are consistent with their frequencies in respective positions.

(B) Heatmap of the amino acid composition around Kla sites. Green indicated the low frequency of an amino acid and red indicated the high frequency.

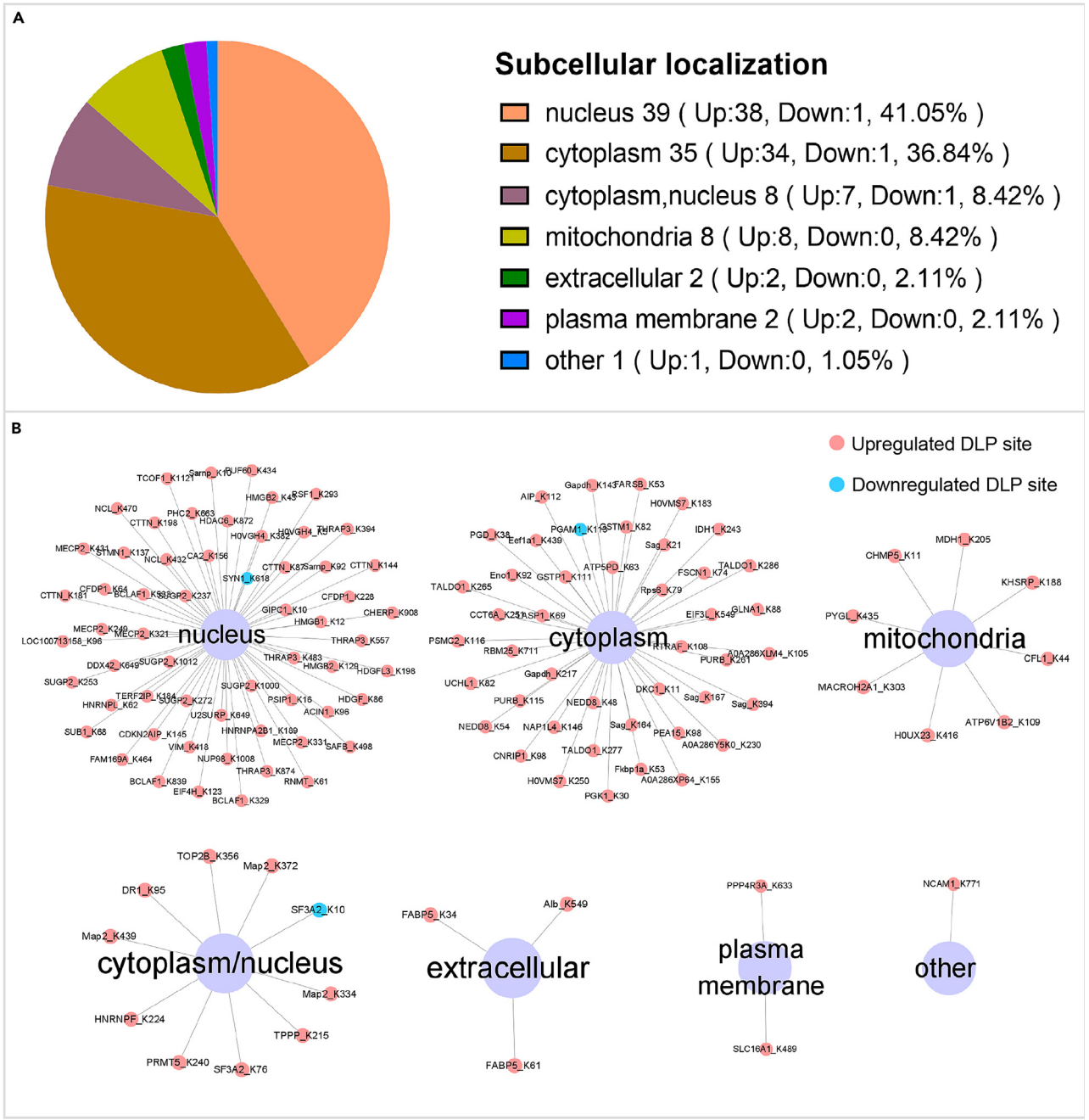

Figure 5. Subcellular localization prediction of DLPs using WoLF PSORT software

(A) The overall distribution of subcellular localization of DLPs.

(B) DLPs in each cell structure, Red circles represent protein sites upregulated with Kla and blue circles represent those downregulated with Kla.

Moreover, several studies have indicated that the catalytic activity of glycolytic enzymes (such as HK, LDHA, and PKM2) can be regulated through protein lysine acetylation modifications.[33–36] For instance, in cirrhosis and hepatocellular carcinoma, deacetylation enhances the glycolytic enzyme activities of GLUT 1, HK, and LDHA.[34] Deacetylation of lysine 305 in PKM2 significantly enhances its enzymatic activity by promoting tetramerization.[35] Another study found that deacetylation of the LDHA lysine 5 site in pancreatic cancer increased protein levels and enzymatic activity.[36] In our previous study, we similarly found that the acetylation levels of HK2, PFK, PKM, and LDHA were significantly downregulated in the retinas of guinea pigs with two-week FDM, which may explain the enhanced protein levels and enzyme activities (Figure 9).[37] As the primary byproduct of the Warburg effect, lactate has long been associated with tumors.[38] However, in our study, we found, for

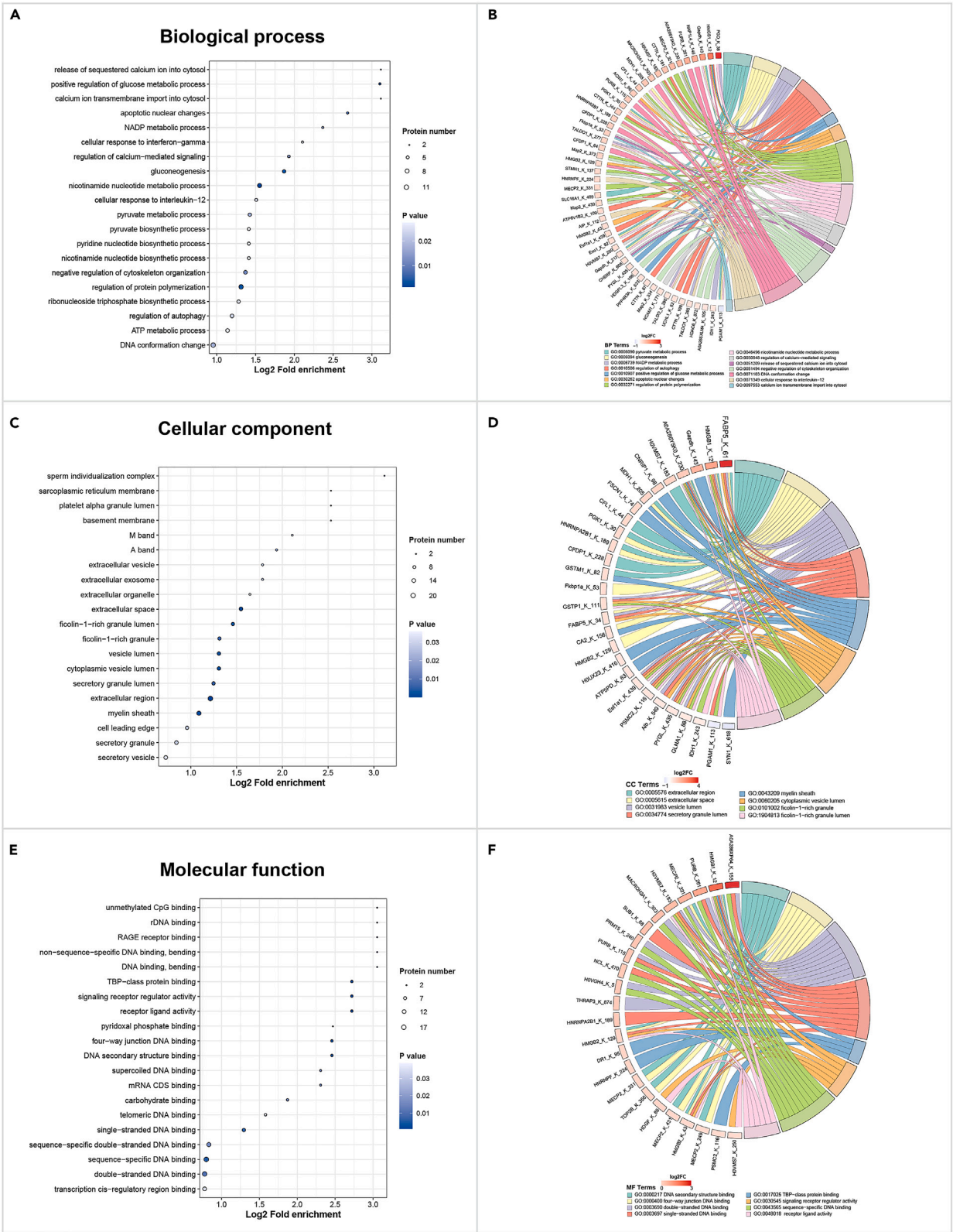
A
Biological process
release of sequestered calcium ion into cytosol
positive regulation of glucose metabolic process
calcium ion transmembrane import into cytosol
apoptotic nuclear changes
NADP metabolic process
cellular response to interferon−gamma
regulation of calcium−mediated signaling
gluconeogenesis
nicotinamide nucleotide metabolic process
cellular response to interleukin−12
pyruvate metabolic process
pyruvate biosynthetic process
pyridine nucleotide biosynthetic process
nicotinamide nucleotide biosynthetic process
negative regulation of cytoskeleton organization
regulation of protein polymerization
ribonucleoside triphosphate biosynthetic process
regulation of autophagy
ATP metabolic process
DNA conformation change
1.0
1.5
2.0
2.5
3.0
Log2 Fold enrichment
Protein number
2
5
8
11
P value
0.02
0.01
B
log2FC
BP Terms
GO:0006090 pyruvate metabolic process
GO:0006094 gluconeogenesis
GO:0009739 NADP metabolic process
GO:0010506 regulation of autophagy
GO:0010907 positive regulation of glucose metabolic process
GO:0030262 apoptotic nuclear changes
GO:0032271 regulation of protein polymerization
GO:0046496 nicotinamide nucleotide metabolic process
GO:0051209 release of sequestered calcium ion into cytosol
GO:0051494 negative regulation of cytoskeleton organization
GO:0071353 cellular response to interleukin−12
GO:0097553 calcium ion transmembrane import into cytosol
C
Cellular component
sperm individualization complex
sarcoplasmic reticulum membrane
platelet alpha granule lumen
basement membrane
M band
A band
extracellular vesicle
extracellular exosome
extracellular organelle
extracellular space
ficolin−1−rich granule lumen
ficolin−1−rich granule
vesicle lumen
cytoplasmic vesicle lumen
secretory granule lumen
extracellular region
myelin sheath
cell leading edge
secretory granule
secretory vesicle
1.0
1.5
2.0
2.5
3.0
Log2 Fold enrichment
Protein number
2
8
14
20
P value
0.03
0.02
0.01
D
log2FC
CC Terms
GO:0005576 extracellular region
GO:0005615 extracellular space
GO:0031983 vesicle lumen
GO:0034774 secretory granule lumen
GO:0043209 myelin sheath
GO:0060205 cytoplasmic vesicle lumen
GO:0101002 ficolin−1−rich granule
GO:1904813 ficolin−1−rich granule lumen
E
Molecular function
unmethylated CpG binding
rDNA binding
RAGE receptor binding
non−sequence−specific DNA binding, bending
DNA binding, bending
TBP−class protein binding
signaling receptor regulator activity
receptor ligand activity
pyridoxal phosphate binding
four−way junction DNA binding
DNA secondary structure binding
supercoiled DNA binding
mRNA CDS binding
carbohydrate binding
telomeric DNA binding
single−stranded DNA binding
sequence−specific double−stranded DNA binding
sequence−specific DNA binding
double−stranded DNA binding
transcription cis−regulatory region binding
1.0
1.5
2.0
2.5
3.0
Log2 Fold enrichment
Protein number
2
7
12
17
P value
0.03
0.02
0.01
F
log2FC
MF Terms
GO:0000217 DNA secondary structure binding
GO:0000400 four−way junction DNA binding
GO:0003690 double−stranded DNA binding
GO:0003697 single−stranded DNA binding
GO:0017025 TBP−class protein binding
GO:0030545 signaling receptor regulator activity
GO:0043565 sequence−specific DNA binding
GO:0048018 receptor ligand activity

Figure 6. GO enrichment analysis of DLPs

(A) Biological process categories.

(B) The relationship between DLPs and biological process categories.

(C) Cellular component.

(D) The relationship between DLPs and Cellular component.

(E) Molecular function.

(F) The relationship between DLPs and Molecular function.

the first time, a significant increase in lactate levels in the retinas of guinea pigs with FDM. Increased glycolytic flux and lactate accumulation are thought to be closely associated with rapid tumor tissue growth, proliferation, and migration.[39,40] This phenomenon was observed in the FDM retina, suggesting that myopic eyes preferentially produce lactate via the glycolytic pathway to meet the energy demands of rapid eye elongation. Recent studies have shown that increased lactate levels can produce more L-lactyl-CoA to mediate protein lysine lactylation modifications.[22] In addition, a novel function of lactate, known as protein lactylation, has been newly proposed as a PTM of proteins to regulate protein function, and Kla has now been found in a few species, including mice,[22] rice,[41] and *Botrytis cinerea*.[42] However, it remains unclear whether changes in lactate content lead to global alterations in protein lactylation levels in the retinas of guinea pigs with FDM. Therefore, in this study, we conducted a comprehensive investigation of Kla levels in the retinal proteins of guinea pigs with FDM.

Significant enhancement of protein lysine lactylation in FDM retinas was first revealed by western blotting and immunofluorescence. Subsequently, 1989 lactylation modification sites on 848 proteins were identified using 4D-lactylation non-label quantitative proteomic analysis, of which 1500 sites on 691 proteins contained quantitative information. We compared form-deprived eyes in the FDM group with the eyes in the NC group. The results revealed that the level of Kla was upregulated at 124 sites on 92 proteins and downregulated at three sites on three proteins in the FDM group compared with that in the NC group. Subcellular localization analysis revealed that DLPs were mainly localized in the nucleus and cytoplasm. Specifically, cytoplasmic glucose undergoes a series of catalytic reactions to produce pyruvate, which is subsequently reduced to lactate by LDH. Lactate catabolism involves two pathways. On the one hand, lactate is oxidized to pyruvate, which enters the mitochondria to undergo the tricarboxylic acid cycle to achieve irreversible lactate clearance; on the other hand, lactate is further converted to lactoyl-CoA, which can either enter the nucleus to participate in the lactylation modification of histone proteins or directly engage in the lactylation modification of non-histone proteins in the cytoplasm.[43,44] Therefore, it is not surprising that subcellular localization analyses showed the DLPs to be primarily located in the nucleus and cytoplasm. The reason for the inconsistency between this result and the enrichment of cellular components in GO enrichment analysis is that the former is based on potential localization predicted from protein sequences whereas the latter provides component enrichment based on functional annotation. The discrepancy between these results highlights the complexity of the possible roles of lactylated proteins in various cellular components.

To further explore the characteristics of the identified DLPs, we analyzed their potential functions using GO and KEGG analyses. GO functional annotation results indicated that the majority of DLPs in eyes with FDM were concentrated in various energy metabolism processes, including the positive regulation of glucose metabolism, NADP metabolism, gluconeogenesis, and cytoplasmic calcium transport, among other biological processes. Interestingly, molecular functional annotation showed that many DLPs were strongly associated with DNA-binding processes. Protein-DNA binding interactions are key to the regulation of gene transcription and are a prerequisite for initiating gene transcription.[45] Although lactylation modifications are strongly associated with transcriptional regulation, lactylation of these proteins may affect the transcription of downstream genes, thereby affecting energy metabolism processes in the retina, which may greatly contribute to the pathogenesis of FDM. Glutathione metabolism, pentose phosphate pathway, HIF-1 signaling pathway, and glycolysis/gluconeogenesis were significantly enriched in the KEGG analysis of the FDM group compared with that of the NC group. The pentose phosphate pathway produces NADPH for the reduction of oxidized glutathione, which is critical for the maintenance of cellular redox homeostasis and the regulation of cellular metabolism.[46] HIF-1 is a major transcription factor involved in tissue metabolism in hypoxic environments and can further regulate the expression of proteins involved in glucose metabolism.[47] Nutrition and oxygen to the retina are supplied by the central retinal artery and choroidal vessels.[48] During the development of myopia, choroidal thinning leads to a decrease in the supply of nutrients and oxygen.[49] However, excessive ocular growth results in a higher requirement for oxygen and nutrition from retinal sources. As a result, the myopic eyes tended to be hypoxic.[50] Our results suggest that lactate is an important substrate for energy metabolism and is involved in the development of myopia under certain conditions by participating in the modification of protein lactylation in these pathways. Therefore, our findings support the hypothesis that the myopic retina is in a state of redox imbalance due to the rapid elongation of the ocular axis and thus needs to utilize glycolysis for rapid energy acquisition.[51] Based on PPI analysis, we found that DLPs were mainly related to the regulation of cellular metabolic processes, nucleic acid metabolic processes, and the production of precursor metabolites and energy. Cells maintain cellular homeostasis and function by coordinating various metabolic processes that provide energy and biosynthetic precursors.[52] The current findings suggest that Kla may influence the development of FDM by affecting cellular metabolic processes in the retina, which confirms the previous results of GO and KEGG enrichment analyses from another angle.

The primary aim of this study was to identify the key proteins that undergo lactylation in the context of FDM and investigate their association with the onset of myopia and the underlying mechanisms. The identification of lactylated proteins may shed light on potential targets for future myopia control. We identified 19 proteins with consistent trends in lactylation modifications by validation using the PRM technique. FABP5 plays a vital role as a lipid chaperone in fatty acids (FAs) transport and metabolism and is closely related to metabolic disorders and abnormal cell proliferation in pathological states.[53] Studies have shown that the intracellular transport of FAs is a complex and dynamic process that directly or indirectly affects various cellular biochemical processes, primarily gene expression, cell development, metabolism, and inflammatory

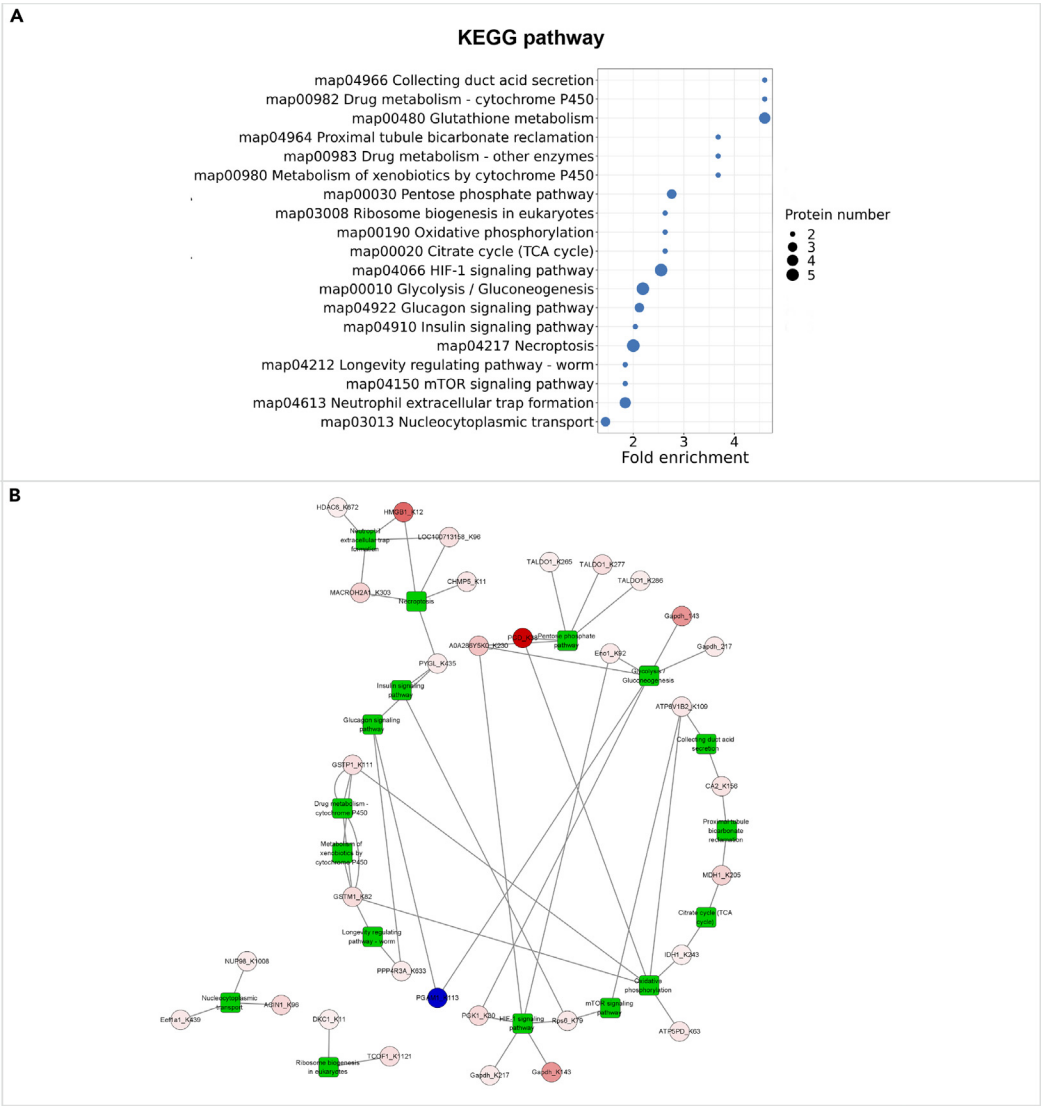

Figure 7. Pathway analysis of DLPs

(A) KEGG pathway enrichment analysis of DLPs.

(B) Significant pathway enrichment of DLPs. Circles represented DLPs, and green boxes indicated different biological. The up-regulated protein was red, while the down-regulated protein was colored blue.

responses.[54] Meanwhile, whether FAs are involved in the development of myopia has attracted attention. A largescale RNA sequencing study by Zeng et al. showed that lipid biosynthetic pathways are significantly downregulated in the retinas of guinea pigs with FDM.[55] Yang et al. used gas chromatography time-of-flight mass spectrometry to detect changes in retinal metabolism during FDM in guinea pigs and found that arachidonic acid was significantly downregulated in the retinas of FDM.[56] In addition, Pan et al. found that the addition of ω-3 polyunsaturated fatty acids (PUFA) to the diet inhibited the decrease in blood flow in the choroid of guinea pigs with FDM and delayed the progression of myopia.[57] Mori et al. used fat-1 mice, which produce endogenous *n*-3 PUFA, as a model and were given an *n*-3 PUFA-free diet. They found that *n*-3 PUFA independently inhibited the development of myopia compared to WT mice lacking *n*-3 PUFA.[58] All of the aforementioned studies suggest that the occurrence of myopia may be associated with a significant downregulation of PUFA; however, the molecular mechanisms underlying the regulation and involvement of these FAs in myopia development remain unclear. Guo et al. found that S-glutathionylation promoted FA binding and nuclear translocation of FABP5, activated PPARβ/δ, and inhibited macrophage inflammation.[59] In our study, elevated levels of Kla at site 61 in FABP5 were found for the first time in myopic retinas, and this finding was confirmed using PRM. Thus, the lactylated modification of FABP5 may be a potential target for myopia treatment, but the underlying mechanism requires further study.

Interestingly, among the validated proteins, glyceraldehyde-3-phosphate dehydrogenase (GAPDH), phosphoglycerate kinase 1 (PGK1), and alpha-enolase 1 (ENO1) are involved in glycolysis. GAPDH, a classical glycolytic enzyme, is one of the most prominent targets of

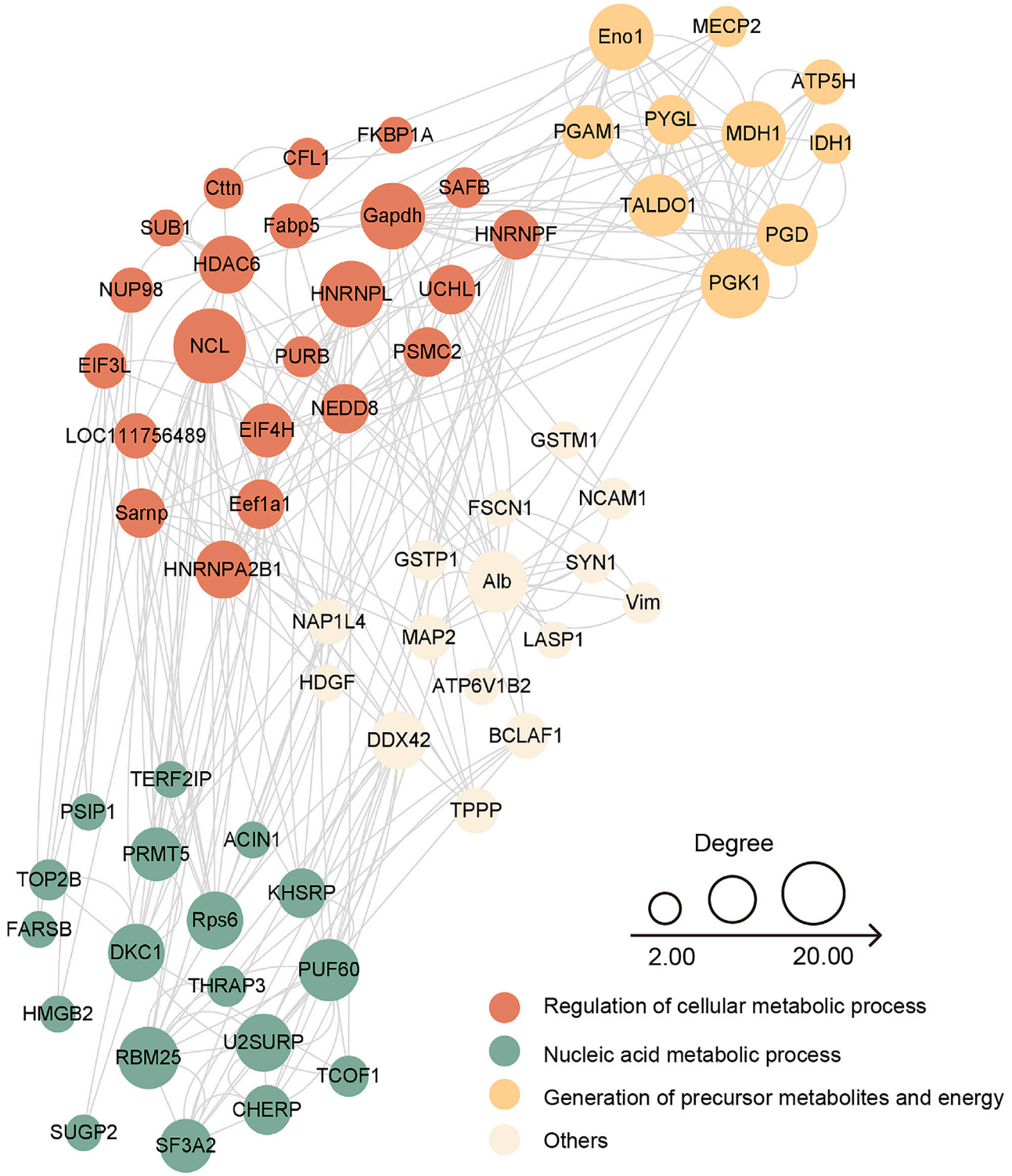

Figure 8. PPI network of DLPs

The size of the nodes indicates the enrichment score. Different colors represent different biological processes: regulation of cellular metabolic processes (red); nucleic acid metabolic process (green); generation of precursor metabolites and energy (yellow); and other biological processes (white).

Table 1. PRM validation results in lactylated proteomic analysis

Protein Accession	Protein Name	Position	FDM/NC Ratio (PRM)	FDM/NC Ratio (4D-LFQ)
A9QUC5	FABP5	K61	1.47	10.17
A0A286XB17	PEA15	K98	1.20	1.53
A0A286XU57	CFL1	K44	1.26	1.66
A0A286XVH5	PURB	K115	1.08	1.47
A4L9L4	SAG	K21	2.04	2.46
B5AN23	GAPDH	K143	1.21	2.80
H0V2B3	EEF1A1	K439	2.66	1.40
H0VU24	THRAP3	K557	1.09	1.45
H0W9D3	GSTP1	K111	1.21	1.67
A0A286XZ92	ATP5PD	K63	1.07	1.44
H0UTZ2	MACROH2A1	K303	1.36	1.80
H0UVC5	VIM	K418	1.47	1.79
H0VBD5	FSCN1	K74	1.25	1.81
H0VYI8	AIP	K112	1.04	1.38
H0W0E9	HNRNPF	K224	1.20	1.43
P16413	GSTM1	K82	1.85	1.55
A0A286XYN2	MDH1	K205	1.44	1.77
A0A286XRU5	PGK1	K30	1.48	1.64
A9YWS9	ENO1	K92	1.68	1.34

Note: PRM, parallel reaction monitoring; 4D-LFQ, 4 dimensions label-free quantitation.

PTMs that alter enzyme activity, subcellular localization, and regulatory interactions with downstream chaperones, thereby affecting glycolytic and non-glycolytic functions.[60–62] GAPDH glutathionylation protects catalytic cysteines from over-oxidation and inactivates the glycolytic function of GAPDH.[60] Increased S-nitrosylation of GAPDH induced by iNOS during aging, followed by its translocation to the nucleus and mediation of apoptosis, leads to age-associated sarcopenia.[61] Acetate enhances GAPDH enzyme activity, aerobic glycolysis, and Th1 cell polarization by modulating GAPDH acetylation levels.[62] PGK1, an important ATP-generating enzyme in glycolysis, is reversibly and dynamically modified at threonine 255 (T255) by O-conjugated N-acetylglucosamine (O-GlcNAc), which activates the activity of PGK1 to enhance glycolysis and acts as a kinase to inhibit pyruvate dehydrogenase activity to inhibit the TCA cycle, thereby promoting tumor growth.[63] Luo et al. found that reduced PGK1 succinylation in a rat model of acute epilepsy may affect the integrity of the blood-brain barrier by altering vasopressin and VEGF levels in the hippocampus, thereby influencing epilepsy.[64] Quan et al. revealed that KIF15 deubiquitinates PGK1 by recruiting USP10, which promotes glycolytic capacity and tumor growth in pancreatic cancer cells.[65] ENO1 is a key glycolytic enzyme, whose aberrant expression drives the pathogenesis of various cancers.[66–68] In a study on oral squamous cell carcinoma, overexpression of NEDD4L led to ubiquitination and subsequent protein degradation of ENO1, which inhibited glycolysis and further inhibited the cell cycle and cell proliferation.[66] Hou et al. showed that lysine crotonylation of ENO1 was significantly elevated in human colorectal cancer tissues, which enhanced its activity and promoted the growth, migration, and invasion of colorectal cancer cells.[67] Yuan et al. reported that aspirin attenuated the glycolysis and proliferation of hepatoma cells by modulating the level of lysine 2-hydroxyisobutyrylation of ENO1.[68] Although the current study found that GAPDH, PGK1, and ENO1 could undergo lactylation in the retinas of FDM, it remains unclear how their lactylation alterations affect their enzymatic activities and functions, which requires further investigation. Here, we show that a feedback loop in the retina may drive the pathogenesis of FDM.[25] After detecting enhanced glycolytic flux and lactate accumulation in the retina of FDM guinea pigs, we found elevated levels of lactylation of the glycolytic enzymes GAPDH, PGK1, and ENO1, which might further promote or inhibit glycolytic metabolism, suggesting that disruption of this feedback loop might be a potential therapeutic approach for myopia.

Glutathione S-transferase pi 1 (GSTP1) and GSTM1 are interesting proteins, both of which are key enzymes involved in the detoxification and metabolism of oxidative stress products.[69] Oxidative stress-induced oxidative damage, resulting from an imbalance between free radical production and antioxidant defense, has been found to be closely associated with various eye diseases, such as glaucoma[70] and cataract.[71] Continuous ocular axis elongation and thinning of scleral thickness in high myopia, along with atrophy of the retinal pigment epithelium and choroid, could lead to oxidative stress in a hypoxic environment.[72] A recent proteomic study of the retinas of FDM rabbits found that oxidative stress in the retina might be closely related to the pathogenesis of myopia.[73] The generation of oxidative stress in the myopic retina under hypoxic conditions is important due to its high blood flow, photo-oxidative damage, and high polyunsaturated FA content, which is one of the most common targets for the generation of free radicals involved in lipid peroxidation products and has been proposed as a marker for the clinical management of many diseases, including myopia.[74] GSTP1 and GSTM1 play key roles in protecting cells from oxidative stress; however, few mechanisms have been studied at the protein modification level. Balchin et al. revealed that S-nitrosylation of Cys47 and Cys101

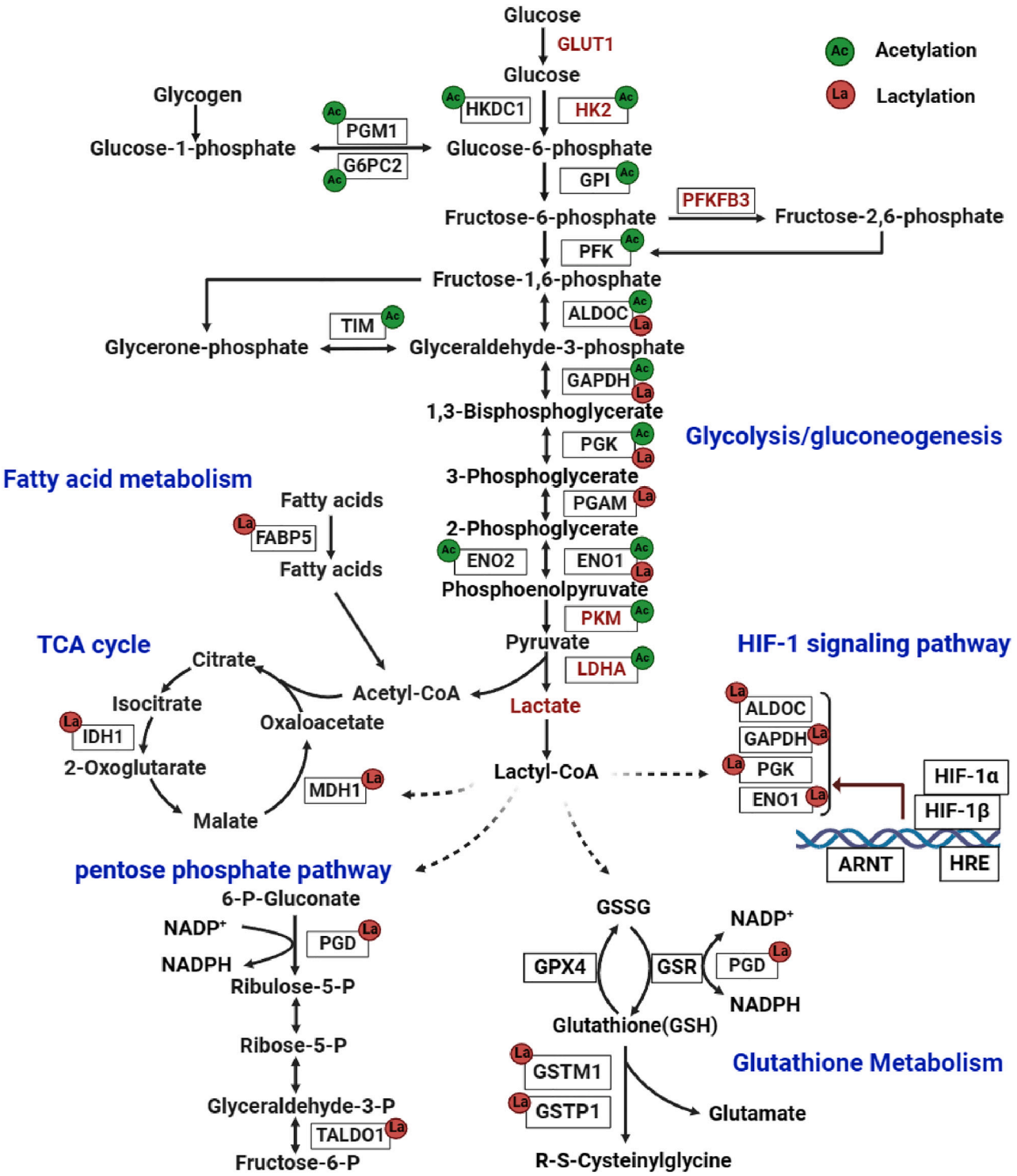

Figure 9. Lactylated enzymes involved in metabolism-related pathways

Proteins marked by red circles are the lactated modifications identified in this study. The green circles mark the acetylation-modified proteins identified in the team's previous studies. Fonts highlighted in red indicate substances for which increased protein expression or activity was detected in this study.

reduced the enzymatic activity of GSTP1 by 94% and destabilized the structural domain of GSTP1.[75] In the present study, we found for the first time that the Kla levels of GSTP1_K111 and GSTM1_K82 were significantly increased in the FDM retinas. However, the effects of lactylation modifications on the activity, structure, stability, and kinetics of these enzymes need to be further investigated to confirm whether they are involved in the progression of myopia by affecting the level of oxidative stress in the myopic retina.

Limitations of the study

The present study has certain limitations. It was limited to the myopic guinea pig retina, and the underlying biological mechanisms by which multiple Kla proteins affect myopia progression have not been thoroughly investigated. Future studies are needed to link retina-choroid-sclera Kla crosstalk to further validate the effects of Kla on protein function and the progression of myopia.

STAR★METHODS

Detailed methods are provided in the online version of this paper and include the following:

- KEY RESOURCES TABLE
- RESOURCE AVAILABILITY
  - Lead contact
  - Materials availability
  - Data and code availability
- EXPERIMENTAL MODEL AND STUDY PARTICIPANT DETAILS
  - Animals and experimental design
- METHOD DETAILS
  - Biological measurements
  - Sample collection and digital capillary western blotting
  - LDH activity and lactate content assay
  - Retinal immunofluorescence
  - Western blotting for mass spectrometry analysis
  - Trypsin digestion and enrichment
  - LC-MS/MS analysis
  - The targeting PRM analysis
  - Bioinformatics analysis
- QUANTIFICATION AND STATISTICAL ANALYSIS

SUPPLEMENTAL INFORMATION

Supplemental information can be found online at https://doi.org/10.1016/j.isci.2024.110606.

ACKNOWLEDGMENTS

This work was supported by the Shandong Traditional Chinese Medicine Science and Technology Program (no. M-2023075), the Focus on Research and Development Plan in Shandong Province (no. 2021LCZX09), the Natural Science Foundation of Shandong Province (no. ZR2021LZY045), and the Shandong Province Integrated Chinese and Western Medicine Specialized Disease Prevention and Treatment Project (no. YXH2019ZXY001).

AUTHOR CONTRIBUTIONS

Conceptualization: J.F., X.C., and J.S.; methodology: J.F. and X.Z.; experimentation: J.F. and R.L.; software: Y.X.; validation: J.F. and X.G.; formal analysis: J.F. and R.L.; investigation: Z.X. and Y.S.; resources: J.S. and H.B.; data curation: J.F. and R.L.; writing – original draft: J.F. and R.L.; writing – review & editing: X.C. and J.S.; visualization: J.F. and Y.X.; supervision: L.Z. and J.S.; funding acquisition: J.S. and H.B. All authors read and approved the final manuscript.

DECLARATION OF INTERESTS

The authors declare that they have no conflict of interest. Each listed author on the manuscript is aware of and agrees to the contents of the manuscript, including the authorship.

Received: November 15, 2023
Revised: May 19, 2024
Accepted: July 25, 2024
Published: July 29, 2024

REFERENCES

1. Modjtahedi, B.S., Ferris, F.L., Hunter, D.G., and Fong, D.S. (2018). Public Health Burden and Potential Interventions for Myopia. Ophthalmology *125*, 628–630. https://doi.org/10.1016/j.ophtha.2018.01.033.
2. Resnikoff, S., Jonas, J.B., Friedman, D., He, M., Jong, M., Nichols, J.J., Ohno-Matsui, K., Smith, E.L., Wildsoet, C.F., Taylor, H.R., et al. (2019). Myopia – A 21st Century Public Health Issue. Invest. Ophthalmol. Vis. Sci. *60*. Mi–Mii. https://doi.org/10.1167/iovs.18-25983.
3. Baird, P.N., Saw, S.-M., Lanca, C., Guggenheim, J.A., Smith III, E.L., Zhou, X., Matsui, K.-O., Wu, P.-C., Sankaridurg, P., Chia, A., et al. (2020). Myopia. Nat. Rev. Dis. Primers *6*, 99. https://doi.org/10.1038/s41572-020-00231-4.
4. Huang, F., Wang, Q., Yan, T., Tang, J., Hou, X., Shu, Z., Wan, F., Yang, Y., Qu, J., and Zhou, X. (2020). The Role of the Dopamine D2 Receptor in Form-Deprivation Myopia in Mice: Studies With Full and Partial D2 Receptor Agonists and Knockouts. Invest. Ophthalmol. Vis. Sci. *61*, 47. https://doi.org/10.1167/iovs.61.6.47.
5. Pollock, L.M., Xie, J., Bell, B.A., and Anand-Apte, B. (2018). Retinoic acid signaling is essential for maintenance of the blood-retinal barrier. FASEB J *32*, 5674–5684. https://doi.org/10.1096/fj.201701469R.
6. Carr, B.J., and Stell, W.K. (2016). Nitric Oxide (NO) Mediates the Inhibition of Form-Deprivation Myopia by Atropine in Chicks. Sci. Rep. *6*, 9. https://doi.org/10.1038/s41598-016-0002-7.
7. Brown, D.M., Mazade, R., Clarkson-Townsend, D., Hogan, K., Datta Roy, P.M., and Pardue, M.T. (2022). Candidate pathways for retina to scleral signaling in refractive eye growth. Exp. Eye Res. *219*, 109071. https://doi.org/10.1016/j.exer.2022.109071.
8. Newcombe, E.A., Delaforge, E., Hartmann-Petersen, R., Skriver, K., and Kragelund, B.B. (2022). How phosphorylation impacts intrinsically disordered proteins and their function. Essays Biochem. *66*, 901–913. https://doi.org/10.1042/EBC20220060.
9. Shvedunova, M., and Akhtar, A. (2022). Modulation of cellular processes by histone and non-histone protein acetylation. Nat. Rev. Mol. Cell Biol. *23*, 329–349. https://doi.org/10.1038/s41580-021-00441-y.
10. Conroy, L.R., Hawkinson, T.R., Young, L.E.A., Gentry, M.S., and Sun, R.C. (2021). Emerging roles of N-linked glycosylation in brain physiology and disorders. Trends Endocrinol. Metab. *32*, 980–993. https://doi.org/10.1016/j.tem.2021.09.006.
11. Li, Y., Li, S., and Wu, H. (2022). Ubiquitination-Proteasome System (UPS) and Autophagy Two Main Protein Degradation Machineries in Response to Cell Stress. Cells *11*, 851. https://doi.org/10.3390/cells11050851.
12. Lu, Y., Song, W., Li, Y., Xiao, J., Du, K., Fu, Q., Zhang, Y., Zhao, L., Yin, Y., Hu, T., and Wen, D. (2022). Mechanisms of NO-Mediated Protein S-Nitrosylation in the Lens-Induced Myopia. Oxid. Med. Cell. Longev. *2022*, 8296043. https://doi.org/10.1155/2022/8296043.
13. Małecki, J.M., Davydova, E., and Falnes, P.Ø. (2022). Protein methylation in mitochondria. J. Biol. Chem. *298*, 101791. https://doi.org/10.1016/j.jbc.2022.101791.
14. Banerjee, S., Wang, Q., Zhao, F., Tang, G., So, C., Tse, D., To, C.-H., Feng, Y., Zhou, X., and Pan, F. (2020). Increased Connexin36 Phosphorylation in AII Amacrine Cell Coupling of the Mouse Myopic Retina. Front. Cell. Neurosci. *14*, 124. https://doi.org/10.3389/fncel.2020.00124.
15. Chen, W., Li, Z., Wang, Q., Wang, Y., and Zhang, Y. (2021). The Role of C-Jun N-terminal Kinase-1 in Controlling Aquaporin-1 and Choroidal Thickness during Recovery from Form-deprivation Myopia in Guinea Pigs. Curr. Eye Res. *46*, 885–894. https://doi.org/10.1080/02713683.2020.1839107.
16. Chen, C.-S., Hsu, Y.-A., Lin, C.-H., Wang, Y.-C., Lin, E.-S., Chang, C.-Y., Chen, J.J.-Y., Wu, M.-Y., Lin, H.-J., and Wan, L. (2022). Fallopia Japonica and Prunella vulgaris inhibit myopia progression by suppressing AKT and NFκB mediated inflammatory reactions. BMC Complement. Med. Ther. *22*, 271. https://doi.org/10.1186/s12906-022-03747-2.
17. Hurley, J.B., Lindsay, K.J., and Du, J. (2015). Glucose, Lactate, and Shuttling of Metabolites in Vertebrate Retinas. J. Neurosci. Res. *93*, 1079–1092. https://doi.org/10.1002/jnr.23583.
18. Fiske, B.P., and Vander Heiden, M.G. (2012). Seeing the Warburg effect in the developing retina. Nat. Cell Biol. *14*, 790–791. https://doi.org/10.1038/ncb2554.
19. Ng, S.K., Wood, J.P.M., Chidlow, G., Han, G., Kittipassorn, T., Peet, D.J., and Casson, R.J. (2015). Cancer-like metabolism of the mammalian retina: Mammalian retina metabolism. Clin. Exp. Ophthalmol. *43*, 367–376. https://doi.org/10.1111/ceo.12462.
20. Vohra, R., Gurubaran, I.S., Henriksen, U., Bergersen, L.H., Rasmussen, L.J., Desler, C., Skytt, D.M., and Kolko, M. (2017). Disturbed mitochondrial function restricts glutamate uptake in the human Müller glia cell line, MIO-M1. Mitochondrion *36*, 52–59. https://doi.org/10.1016/j.mito.2017.02.003.
21. Du, J., Cleghorn, W., Contreras, L., Linton, J.D., Chan, G.C.-K., Chertov, A.O., Saheki, T., Govindaraju, V., Sadilek, M., Satrústegui, J., and Hurley, J.B. (2013). Cytosolic reducing power preserves glutamate in retina. Proc. Natl. Acad. Sci. USA *110*, 18501–18506. https://doi.org/10.1073/pnas.1311193110.
22. Zhang, D., Tang, Z., Huang, H., Zhou, G., Cui, C., Weng, Y., Liu, W., Kim, S., Lee, S., Perez-Neut, M., et al. (2019). Metabolic regulation of gene expression by histone lactylation. Nature *574*, 575–580. https://doi.org/10.1038/s41586-019-1678-1.
23. Cui, H., Xie, N., Banerjee, S., Ge, J., Jiang, D., Dey, T., Matthews, Q.L., Liu, R.-M., and Liu, G. (2021). Lung Myofibroblasts Promote Macrophage Profibrotic Activity through Lactate-induced Histone Lactylation. Am. J. Respir. Cell Mol. Biol. *64*, 115–125. https://doi.org/10.1165/rcmb.2020-0360OC.
24. Gaffney, D.O., Jennings, E.Q., Anderson, C.C., Marentette, J.O., Shi, T., Schou Oxvig, A.M., Streeter, M.D., Johannsen, M., Spiegel, D.A., Chapman, E., et al. (2020). Non-Enzymatic Lysine Lactoylation of Glycolytic Enzymes. Cell Chem. Biol. *27*, 206–213.e6. https://doi.org/10.1016/j.chembiol.2019.11.005.
25. Pan, R.-Y., He, L., Zhang, J., Liu, X., Liao, Y., Gao, J., Liao, Y., Yan, Y., Li, Q., Zhou, X., et al. (2022). Positive feedback regulation of microglial glucose metabolism by histone H4 lysine 12 lactylation in Alzheimer's disease. Cell Metab. *34*, 634–648.e6. https://doi.org/10.1016/j.cmet.2022.02.013.
26. Yang, K., Fan, M., Wang, X., Xu, J., Wang, Y., Tu, F., Gill, P.S., Ha, T., Liu, L., Williams, D.L., and Li, C. (2022). Lactate promotes macrophage HMGB1 lactylation, acetylation, and exosomal release in polymicrobial sepsis. Cell Death Differ. *29*, 133–146. https://doi.org/10.1038/s41418-021-00841-9.
27. Wang, X., Fan, W., Li, N., Ma, Y., Yao, M., Wang, G., He, S., Li, W., Tan, J., Lu, Q., and Hou, S. (2023). YY1 lactylation in microglia promotes angiogenesis through transcription activation-mediated upregulation of FGF2. Genome Biol. *24*, 87. https://doi.org/10.1186/s13059-023-02931-y.
28. Schaeffel, F., and Feldkaemper, M. (2015). Animal models in myopia research. Clin. Exp. Optom. *98*, 507–517. https://doi.org/10.1111/cxo.12312.
29. Haydinger, C.D., Kittipassorn, T., and Peet, D.J. (2020). Power to see—Drivers of aerobic glycolysis in the mammalian retina: A review. Clin. Exp. Ophthalmol. *48*, 1057–1071. https://doi.org/10.1111/ceo.13833.
30. Barathi, V.A., Chaurasia, S.S., Poidinger, M., Koh, S.K., Tian, D., Ho, C., Iuvone, P.M., Beuerman, R.W., and Zhou, L. (2014). Involvement of GABA Transporters in Atropine-Treated Myopic Retina As Revealed by iTRAQ Quantitative Proteomics. J. Proteome Res. *13*, 4647–4658. https://doi.org/10.1021/pr500558y.
31. Zhu, Y., Bian, J.F., Lu, D.Q., To, C.H., Lam, C.S.-Y., Li, K.K., Yu, F.J., Gong, B.T., Wang, Q., Ji, X.W., et al. (2022). Alteration of EIF2 Signaling, Glycolysis, and Dopamine Secretion in Form-Deprived Myopia in Response to 1% Atropine Treatment: Evidence From Interactive iTRAQ-MS and SWATH-MS Proteomics Using a Guinea Pig Model. Front. Pharmacol. *13*, 814814. https://doi.org/10.3389/fphar.2022.814814.
32. Yu, F.-J., Lam, T.C., Sze, A.Y.-H., Li, K.-K., Chun, R.K.-M., Shan, S.-W., and To, C.-H. (2020). Alteration of retinal metabolism and oxidative stress may implicate myopic eye growth: Evidence from discovery and targeted proteomics in an animal model. J. Proteomics *221*, 103684. https://doi.org/10.1016/j.jprot.2020.103684.
33. Wu, H., Huang, H., and Zhao, Y. (2023). Interplay between metabolic reprogramming and post-translational modifications: from glycolysis to lactylation. Front. Immunol. *14*, 1211221. https://doi.org/10.3389/fimmu.2023.1211221.
34. Li, J., Wang, T., Xia, J., Yao, W., and Huang, F. (2019). Enzymatic and nonenzymatic protein acetylations control glycolysis process in liver diseases. FASEB J *33*, 11640–11654. https://doi.org/10.1096/fj.201901175R.
35. Park, S.-H., Ozden, O., Liu, G., Song, H.Y., Zhu, Y., Yan, Y., Zou, X., Kang, H.-J., Jiang, H., Principe, D.R., et al. (2016). SIRT2-mediated deacetylation and tetramerization of pyruvate kinase directs glycolysis and tumor growth. Cancer Res. *76*, 3802–3812. https://doi.org/10.1158/0008-5472.CAN-15-2498.
36. Zhao, D., Xiong, Y., Lei, Q.-Y., and Guan, K.-L. (2013). LDH-A Acetylation: Implication in Cancer. Oncotarget *4*, 802–803.
37. Feng, J., Zhang, X., Li, R., Zhao, P., Han, X., Wu, Q., Tian, Q., Tang, G., Song, J., and Bi, H. (2023). Widespread Involvement of Acetylation in the Retinal Metabolism of Form-Deprivation Myopia in Guinea Pigs. ACS Omega *8*, 23825–23839. https://doi.org/10.1021/acsomega.3c02219.
38. Tasdogan, A., Faubert, B., Ramesh, V., Ubellacker, J.M., Shen, B., Solmonson, A.,

Murphy, M.M., Gu, Z., Gu, W., Martin, M., et al. (2020). Metabolic heterogeneity confers differences in melanoma metastatic potential. Nature *577*, 115–120. https://doi.org/10.1038/s41586-019-1847-2.

39. Yang, J., Ren, B., Yang, G., Wang, H., Chen, G., You, L., Zhang, T., and Zhao, Y. (2020). The enhancement of glycolysis regulates pancreatic cancer metastasis. Cell. Mol. Life Sci. *77*, 305–321. https://doi.org/10.1007/s00018-019-03278-z.
40. Abbaszadeh, Z., Çeşmeli, S., and Biray Avcı, Ç. (2020). Crucial players in glycolysis: Cancer progress. Gene *726*, 144158. https://doi.org/10.1016/j.gene.2019.144158.
41. Meng, X., Baine, J.M., Yan, T., and Wang, S. (2021). Comprehensive Analysis of Lysine Lactylation in Rice (*Oryza sativa*) Grains. J. Agric. Food Chem. *69*, 8287–8297. https://doi.org/10.1021/acs.jafc.1c00760.
42. Gao, M., Zhang, N., and Liang, W. (2020). Systematic Analysis of Lysine Lactylation in the Plant Fungal Pathogen Botrytis cinerea. Front. Microbiol. *11*, 594743. https://doi.org/10.3389/fmicb.2020.594743.
43. Li, X., Yang, Y., Zhang, B., Lin, X., Fu, X., An, Y., Zou, Y., Wang, J.-X., Wang, Z., and Yu, T. (2022). Lactate metabolism in human health and disease. Signal Transduct. Target. Ther. *7*, 305. https://doi.org/10.1038/s41392-022-01151-3.
44. Rabinowitz, J.D., and Enerbäck, S. (2020). Lactate: the ugly duckling of energy metabolism. Nat. Metab. *2*, 566–571. https://doi.org/10.1038/s42255-020-0243-4.
45. Hocek, M. (2019). Enzymatic Synthesis of Base-Functionalized Nucleic Acids for Sensing, Cross-linking, and Modulation of Protein–DNA Binding and Transcription. Acc. Chem. Res. *52*, 1730–1737. https://doi.org/10.1021/acs.accounts.9b00195.
46. Xiao, W., and Loscalzo, J. (2020). Metabolic Responses to Reductive Stress. Antioxid. Redox Signal. *32*, 1330–1347. https://doi.org/10.1089/ars.2019.7803.
47. Zhang, Z., Yao, L., Yang, J., Wang, Z., and Du, G. (2018). PI3K/Akt and HIF-1 signaling pathway in hypoxia-ischemia. Mol. Med. Rep. *18*, 3547–3554. https://doi.org/10.3892/mmr.2018.9375.
48. Behar-Cohen, F., Gelizé, E., Jonet, L., and Lassiaz, P. (2020). Anatomie de la rétine. Med. Sci. *36*, 594–599. https://doi.org/10.1051/medsci/2020094.
49. Liu, Y., Wang, L., Xu, Y., Pang, Z., and Mu, G. (2021). The influence of the choroid on the onset and development of myopia: from perspectives of choroidal thickness and blood flow. Acta Ophthalmol. *99*, 730–738. https://doi.org/10.1111/aos.14773.
50. Wu, H., Chen, W., Zhao, F., Zhou, Q., Reinach, P.S., Deng, L., Ma, L., Luo, S., Srinivasalu, N., Pan, M., et al. (2018). Scleral hypoxia is a target for myopia control. Proc. Natl. Acad. Sci. USA *115*, E7091–E7100. https://doi.org/10.1073/pnas.1721443115.
51. Kierans, S.J., and Taylor, C.T. (2021). Regulation of glycolysis by the hypoxia-inducible factor (HIF): implications for cellular physiology. J. Physiol. *599*, 23–37. https://doi.org/10.1113/JP280572.
52. Mesquita, I., and Rodrigues, F. (2018). Cellular Metabolism at a Glance. In Metabolic Interaction in Infection Experientia Supplementum, R. Silvestre and E. Torrado, eds. (Springer International Publishing), pp. 3–27. https://doi.org/10.1007/978-3-319-74932-7_1.
53. Wang, G., Bonkovsky, H.L., de Lemos, A., and Burczynski, F.J. (2015). Recent insights into the biological functions of liver fatty acid binding protein 1. J. Lipid Res. *56*, 2238–2247. https://doi.org/10.1194/jlr.R056705.
54. Koundouros, N., and Poulogiannis, G. (2020). Reprogramming of fatty acid metabolism in cancer. Br. J. Cancer *122*, 4–22. https://doi.org/10.1038/s41416-019-0650-z.
55. Zeng, L., Li, X., Liu, J., Liu, H., Xu, H., and Yang, Z. (2021). RNA-Seq Analysis Reveals an Essential Role of the Tyrosine Metabolic Pathway and Inflammation in Myopia-Induced Retinal Degeneration in Guinea Pigs. Int. J. Mol. Sci. *22*, 12598. https://doi.org/10.3390/ijms222212598.
56. Yang, J., Reinach, P.S., Zhang, S., Pan, M., Sun, W., Liu, B., Li, F., Li, X., Zhao, A., Chen, T., et al. (2017). Changes in retinal metabolic profiles associated with form deprivation myopia development in guinea pigs. Sci. Rep. *7*, 2777. https://doi.org/10.1038/s41598-017-03075-3.
57. Pan, M., Zhao, F., Xie, B., Wu, H., Zhang, S., Ye, C., Guan, Z., Kang, L., Zhang, Y., Zhou, X., et al. (2021). Dietary ω-3 polyunsaturated fatty acids are protective for myopia. Proc. Natl. Acad. Sci. USA *118*, e2104689118. https://doi.org/10.1073/pnas.2104689118.
58. Mori, K., Kuroha, S., Hou, J., Jeong, H., Ogawa, M., Ikeda, S.I., Kang, J.X., Negishi, K., Torii, H., Arita, M., et al. (2022). Lipidomic analysis revealed n-3 polyunsaturated fatty acids suppressed choroidal thinning and myopia progression in mice. Faseb. J. *36*, e22312. https://doi.org/10.1096/fj.202101947R.
59. Guo, Y., Liu, Y., Zhao, S., Xu, W., Li, Y., Zhao, P., Wang, D., Cheng, H., Ke, Y., and Zhang, X. (2021). Oxidative stress-induced FABP5 S-glutathionylation protects against acute lung injury by suppressing inflammation in macrophages. Nat. Commun. *12*, 7094. https://doi.org/10.1038/s41467-021-27428-9.
60. Tossounian, M.-A., Zhang, B., and Gout, I. (2020). The Writers, Readers, and Erasers in Redox Regulation of GAPDH. Antioxidants *9*, 1288. https://doi.org/10.3390/antiox9121288.
61. Xie, T., Qiao, X., Sun, C., Chu, B., Meng, J., and Chen, C. (2022). GAPDH S-nitrosation contributes to age-related sarcopenia through mediating apoptosis. Nitric Oxide *120*, 1–8. https://doi.org/10.1016/j.niox.2021.12.006.
62. Jing, X., Lyu, J., and Xiong, J. (2023). Acetate regulates GAPDH acetylation and T helper 1 cell differentiation. Mol. Biol. Cell *34*, br10. https://doi.org/10.1091/mbc.E23-02-0070.
63. Nie, H., Ju, H., Fan, J., Shi, X., Cheng, Y., Cang, X., Zheng, Z., Duan, X., and Yi, W. (2020). O-GlcNAcylation of PGK1 coordinates glycolysis and TCA cycle to promote tumor growth. Nat. Commun. *11*, 36. https://doi.org/10.1038/s41467-019-13601-8.
64. He, Y., Luo, Y., Zhang, D., Wang, X., Zhang, P., Li, H., Ejaz, S., and Liang, S. (2019). PGK1-mediated cancer progression and drug resistance. Am. J. Cancer Res. *9*, 2280–2302.
65. Quan, G., Xu, J., Wang, J., Liu, X., Xu, J., and Jiang, J. (2023). KIF15 is essential for USP10-mediated PGK1 deubiquitination during the glycolysis of pancreatic cancer. Cell Death Dis. *14*, 137. https://doi.org/10.1038/s41419-023-05679-2.
66. Zhang, G., Zhao, X., and Liu, W. (2022). NEDD4L inhibits glycolysis and proliferation of cancer cells in oral squamous cell carcinoma by inducing ENO1 ubiquitination and degradation. Cancer Biol. Ther. *23*, 243–253. https://doi.org/10.1080/15384047.2022.2054244.
67. Hou, J.-Y., Cao, J., Gao, L.-J., Zhang, F.-P., Shen, J., Zhou, L., Shi, J.-Y., Feng, Y.-L., Yan, Z., Wang, D.-P., and Cao, J.M. (2021). Upregulation of α enolase (ENO1) crotonylation in colorectal cancer and its promoting effect on cancer cell metastasis. Biochem. Biophys. Res. Commun. *578*, 77–83. https://doi.org/10.1016/j.bbrc.2021.09.027.
68. Yuan, Y., Yuan, H.F., Geng, Y., Zhao, L.N., Yun, H.L., Wang, Y.F., Yang, G., and Zhang, X.D. (2021). Aspirin modulates 2-hydroxyisobutyrylation of ENO1K281 to attenuate the glycolysis and proliferation of hepatoma cells. Biochem. Biophys. Res. Commun. *560*, 172–178. https://doi.org/10.1016/j.bbrc.2021.04.083.
69. Kelly, F.J., and Fussell, J.C. (2017). Role of oxidative stress in cardiovascular disease outcomes following exposure to ambient air pollution. Free Radic. Biol. Med. *110*, 345–367. https://doi.org/10.1016/j.freeradbiomed.2017.06.019.
70. Li, S., Shao, M., Li, Y., Li, X., Wan, Y., Sun, X., and Cao, W. (2020). Relationship between Oxidative Stress Biomarkers and Visual Field Progression in Patients with Primary Angle Closure Glaucoma. Oxid. Med. Cell. Longev. *2020*, 2701539. https://doi.org/10.1155/2020/2701539.
71. Richardson, R.B., Ainsbury, E.A., Prescott, C.R., and Lovicu, F.J. (2020). Etiology of posterior subcapsular cataracts based on a review of risk factors including aging, diabetes, and ionizing radiation. Int. J. Radiat. Biol. *96*, 1339–1361. https://doi.org/10.1080/09553002.2020.1812759.
72. Mérida, S., Villar, V.M., Navea, A., Desco, C., Sancho-Tello, M., Peris, C., and Bosch-Morell, F. (2020). Imbalance Between Oxidative Stress and Growth Factors in Human High Myopia. Front. Physiol. *11*, 463. https://doi.org/10.3389/fphys.2020.00463.
73. Moon, C.-E., Ji, Y.W., Lee, J.K., Han, K., Kim, H., Byeon, S.H., Han, S., Han, J., and Seo, Y. (2023). Retinal Proteome Analysis Reveals a Region-Specific Change in the Rabbit Myopia Model. Int. J. Mol. Sci. *24*, 1286. https://doi.org/10.3390/ijms24021286.
74. Francisco, B.-M., Salvador, M., and Amparo, N. (2015). Oxidative Stress in Myopia. Oxid. Med. Cell. Longev. *2015*, 750637. https://doi.org/10.1155/2015/750637.
75. Balchin, D., Stoychev, S.H., and Dirr, H.W. (2013). S- Nitrosation Destabilizes Glutathione Transferase P1-1. Biochemistry *52*, 9394–9402. https://doi.org/10.1021/bi401414c.
76. Zhou, X., Qu, J., Xie, R., Wang, R., Jiang, L., Zhao, H., Wen, J., and Lu, F. (2006). Normal development of refractive state and ocular dimensions in guinea pigs. Vision Res. *46*, 2815–2823. https://doi.org/10.1016/j.visres.2006.01.027.
77. Yang, Z., Yan, C., Ma, J., Peng, P., Ren, X., Cai, S., Shen, X., Wu, Y., Zhang, S., Wang, X., et al. (2023). Lactylome analysis suggests lactylation-dependent mechanisms of metabolic adaptation in hepatocellular carcinoma. Nat. Metab. *5*, 61–79. https://doi.org/10.1038/s42255-022-00710-w.

STAR★METHODS

KEY RESOURCES TABLE

REAGENT or RESOURCE	SOURCE	IDENTIFIER
Antibodies		
Anti-GLUT1 antibody	Proteintech	Cat#21829-1-AP; RRID:AB_10837075
Anti-PFKFB3 antibody	Proteintech	Cat# 13763-1-AP; RRID:AB_2162854
Anti-PKM antibody	Proteintech	Cat# 10078-2-AP; RRID:AB_2283775
Anti-LDHA antibody	Proteintech	Cat# 21799-1-AP; RRID:AB_10858925
Anti-β-Actin	PTM Bio	Cat# PTM-5018; RRID:AB_3086678
Anti-HK2 antibody	ABclonal	Cat# A20829; RRID:AB_3066055
Anti-L-Lactyl Lysine	PTM Bio	Cat# PTM-1401RM; RRID:AB_2942013
Goat anti-Rabbit IgG (H + L) Secondary Antibody	Thermo Fisher	Cat# 31460; RRID: AB_228341
Chemicals, peptides, and recombinant proteins		
Proteinase K	Sparkjade	Cat# AC1201
Endogenous peroxidase occlusion solution	Sparkjade	Cat# EE0007
FAS eyeball fixative solution	Servicebio	Cat# G1109
Urea	Sigma-Aldrich	Cat# V900119
Polyvinylidene fluoride	Millipore	Cat# ISEQ00010
SDS	Solarbio	Cat# S8010
EDTA	Sigma-Aldrich	Cat# V900081
Dithiothreitol	Sigma-Aldrich	Cat# D9163
Iodoacetamide	Sigma-Aldrich	Cat# V900335
C18 ZipTips	Millipore	Cat# ZTC18M096
Formic acid	Fluka	Cat# A117-50
Acetonitrile	ThermoFisher	Cat# 204433
NP-40	Solarbio	Cat# N8030
IMAC	ThermoFisher	Cat# A32992
Coomassie brilliant blue	Macklin	Cat# B802270
Trypsin	Promega	Cat# V5280
Trifluoroacetic acid	Sigma-Aldrich	Cat# 302031
Critical commercial assays		
BCA protein assay kit	Beyotime Bio	Cat# P0012
LDH activity assay kit	Solarbio	Cat# BC0685
Lactate assay kit	Solarbio	Cat# BC2235
ECL chemiluminescence kit	Millipore	Cat# WBKLS0500
Jess/Wes Separation Capillary Cartridges	ProteinSimple	Cat# SM-W004
Chemiluminescent Substrate	ProteinSimple	Cat# PS-CS01
Deposited data		
Mass spectrometry protomics data	This paper	[PRIDE]: PXD046495
Software and algorithms		
GraphPad Prism 8	GraphPad software	v.8.0.2
SPSS	SPSS software	v.25.0
Compass	Compass software	v.6.1.0
Cytoscape	Cytoscape software	v.3.9.1

(*Continued on next page*)

Continued

REAGENT or RESOURCE	SOURCE	IDENTIFIER
MaxQuant	www.maxquant.org/	v.1.6.15.0
Eggnog-mapper	http://eggnog5.embl.de/#/app/home	v.2.1.6
PfamScan	https://www.ebi.ac.uk/interpro/entry/pfam/#table	v.1.6
Diamond	http://www.kegg.jp/kegg/mapper.html	v.2.0.11.149
Wolf Psort	www.genscript.com/psort/wolf_psort.html	v.0.2
STRING database	https://string-db.org/	v.11.5

RESOURCE AVAILABILITY

Lead contact

Further information and requests for resources and reagents should be directed to and will be fulfilled by the lead contact, Hongsheng Bi (hongshengbi1@163.com).

Materials availability

This study did not generate new unique reagents.

Data and code availability

- The lactylome data have been deposited in the ProteomeXchange dataset (PRIDE) under the accession number PXD046495.
- This paper does not report the original code.
- Any additional information required to reanalyze the data reported in this paper is available from the lead contact upon request.

EXPERIMENTAL MODEL AND STUDY PARTICIPANT DETAILS

Animals and experimental design

Sixty healthy 2-week-old male pigmented guinea pigs (Cavia porcellus, 110–120 g) were purchased from Henan Kangda Laboratory Animal Ltd. and maintained at the Animal Experimental Center of the Affiliated Eye Hospital of Shandong University of Traditional Chinese Medicine. All animals were randomly assigned to either the 2-week monocular FDM group or the 2-week NC group (30 animals per group). Fresh vegetables and water were freely available. The animal room was exposed to a 12 h light/dark cycle. The light illumination in the cages was approximately 350 lux. No eyes in the NC group received treatment. In the monocular FDM group, the 3D-printed hoods used for the animal experiments were modified by a latex balloon with 60% light transmission that covered the guinea pigs' right eye, leaving the left eye, nose, mouth, and ears exposed (Figure 1C).[37] Hoods were checked and repositioned daily for completeness and cleanliness, and replaced immediately with new hoods of appropriate size, if necessary.

This study was approved by the Animal Care and Ethics Committee of the Affiliated Eye Hospital of Shandong University of Traditional Chinese Medicine, Jinan, China. All procedures were performed in accordance with the Association for Research in Vision and the Ophthalmology Statement for the Use of Animals in Ophthalmic and Vision Research.

METHOD DETAILS

Biological measurements

Refraction and AL measurements were taken at the beginning and end of the treatment period, as described previously.[37] Biometric measurements were performed by a research optometrist who was blinded to the treatment group assignment, with the help of an animal care assistant. Briefly, one drop of compound tropicamide phenylephrine eye drops (Santen, Japan) was injected into the conjunctival sac of guinea pigs every 5 min for three consecutive times, and then they were left for 30 min in a dark room. The optometrist measured the refraction of the guinea pigs in a dark room using a streak retinoscope (YZ24; 66 Vision Technology Co., Ltd., China). The average of the vertical and horizontal meridians was used as the equivalent refraction, and the average of the three measurements was calculated.

The AL was measured using A-scan ultrasonography (Cinescan, Quantel Medical, France), with instrument parameters adjusted for the guinea pigs. The conducting velocities of the anterior chamber, lens, and vitreous chambers were 1557, 1723, and 1540 m/s, respectively.[76] Local anesthesia of the ocular surface was performed using oxybuprocaine hydrochloride (Santen, Japan). The final AL values were obtained from the mean of 10 replicate measurements. The hoods of the guinea pigs in the FDM group were removed and cleaned before each measurement and put back on immediately after completion of the measurement.

Sample collection and digital capillary western blotting

After form deprivation for two weeks, all guinea pigs were euthanized by intraperitoneal injection of an overdose of pentobarbital sodium solution (100 mg/kg). The form-deprived eye in the FDM group and the right eye in the NC group were removed. As shown in Figure 1C, the peripapillary blood vessels and muscles were first clipped, and the eyeball was sheared circularly along the corneoscleral limbus 1 mm below the limbus. The anterior part of the eye and the vitreous body were discarded, and the neurosensory layer of the retina, which contained almost no retinal pigment epithelial layer, was carefully separated. The retinas were then frozen in liquid nitrogen and stored at −80°C until use.

The protein expression levels of GLUT1, HK2, PFKFB3, PKM, LDHA, and β-actin were assayed using a ProteinSimple Abby capillary western blotting analyzer (ProteinSimple, CA, USA). Three retinas per group were randomly selected for protein extraction, and a mixture of RIPA lysis buffer and PMSF protease inhibitor was added to each tissue at a ratio of 10 mg: 100 μL. The tissues were then thoroughly ground at 4°C, and the supernatants were collected after centrifugation at 8000 rpm for 5 min, and the protein concentration was measured using a BCA protein assay kit (Beyotime Bio, Shanghai, China). Each sample was dissolved in PBS (1X) solution to a final up-sampling concentration of 2 μg/μL. Western blotting was performed using the Abby system, according to the manufacturer's protocol. Primary antibodies were GLUT1 (1:150; 21829-1-AP, Proteintech Bio, Wuhan, China), HK2 (1:35; A20829, ABclonal, Wuhan, China), PFKFB3 (1:50; 13763-2-AP, Proteintech Bio, Wuhan, China), PKM (1:50; 10078- 2-AP, Proteintech Bio, Wuhan, China), LDHA (1:50; 21799-2-AP, Proteintech Bio, Wuhan, China), and β-actin (1:50; PTM-5018, PTM Bio, Hangzhou, China). The bands were quantitatively analyzed using Compass software (v6.1.0).

LDH activity and lactate content assay

Five and six randomly selected retinas from each group were assessed for LDH activity and lactate production, respectively. Briefly, the corresponding tissue extract was added to the retinal tissue, which was ground, and the supernatant was collected after centrifugation. LDH activity and lactate content were measured using an LDH activity assay kit (BC0685, Solarbio, Beijing, China) and a lactate assay kit (BC2235, Solarbio, Beijing, China), respectively, and the corresponding optical densities were measured at 450 nm (LDH) and 570 nm (lactate) using an enzyme-linked immunosorbent assay reader according to the manufacturer's instructions. Finally, the LDH activity and lactate content were calculated according to the manufacturer's instructions.

Retinal immunofluorescence

Three eyes from each group were examined for immunofluorescence staining. The eyes were placed on an ice box immediately after removal. We operated under a microscope using ophthalmic surgical scissors and forceps. After carefully lifting and stripping the blood vessels and muscle tissue around the eyeball, the eyeball was quickly immersed in a 4°C FAS eyeball fixative (Servicebio, Wuhan, China) for more than 24 h. Subsequently, the eyes were paraffin-embedded and cut into 5-μm-thick slices, which were allowed to dry and then deparaffinized in an oven at 65°C for 60 min. Tissue sections were immersed in xylene three times (7 min each), twice in 100% ethanol (5 min each), sequentially in a graded ethanol solution for 5 min each (95%, 85%, 75%, and 50%), and finally in ultrapure water for 5 min. Proteinase K antigen repair solution (Sparkjade, Shandong, China) was added dropwise to the tissue sections, and antigen repair was carried out at 37°C for 30 min in the oven, naturally cooled to room temperature, and washed with PBS three times for 5 min each. Endogenous peroxidase sealing solution (Sparkjade, Shandong, China) was added dropwise to the sections, which were closed at room temperature for 10 min to remove endogenous peroxidase and washed again. Sections were blocked with goat serum sealer for 30 min in a 37°C oven and incubated overnight at 4°C with anti-lactyl-lysine antibody (1:50; PTM-1401RM, PTM Bio). After washing three times with PBS, the sections were incubated with Alexa Fluor 488 goat anti-rabbit secondary antibody for 1 h at room temperature. After washing three more times, the retina was sealed with DAPI. Images were captured using a Leica DM IL LED fluorescent inverted microscope at 200× magnification. The mean optical density values of the retina were measured using the ImageJ software.

Western blotting for mass spectrometry analysis

Six retinal tissues from each group were used for protein extraction. The extraction procedure was consistent with our previously described method.[37] Each well was supersampled with 15 μg of protein lysate, and the electrophoresis buffer enabled the bands to be separated and transferred to a polyvinylidene difluoride membrane. Membranes were blocked with 5% skim milk for 1 h at room temperature, followed by overnight incubation at 4°C in anti-lactyl-lysine antibody (1:300; PTM-1401RM, PTM Bio). The next day, the membranes were washed three times (10 min each) with TBST and incubated with horseradish peroxidase-conjugated secondary antibody (1:10,000; 31460, Thermo) for 2 h at 4°C. The membranes were washed with TBST three times (10 min per wash). Protein bands were visualized using an ECL chemiluminescence kit (WBKLS0500; Millipore).

Trypsin digestion and enrichment

The total retinal protein extraction method was the same as previously described. When digesting, 20% trichloroacetic acid was added to the protein solution, vortexed and mixed well, and precipitated at 4°C for 2 h. Centrifuged at 4,500 g for 5 min, the supernatant was discarded and the precipitate was washed three times with pre-cooled acetone. After the precipitate dried, tetraethylammonium bromide was added at a final concentration of 200 mM and dispersed by ultrasonication. The first digestion was performed overnight by adding trypsin at a 1:50

trypsin-to-protein volume ratio. The samples were reduced with 5 mM dithiothreitol at 56°C for 30 min. Finally, iodoacetamide was added to a final concentration of 11 mM and incubated for 15 min at room temperature in the dark.

The enrichment method for the lysine lactylation-modified peptides was consistent with that described by Yang et al.[77] Briefly, tryptic peptides dissolved in IP buffer were incubated with prewashed antibody beads overnight at 4°C with gentle shaking. The antibody beads were washed, and the bound peptides were eluted with 0.1% trifluoroacetic acid. Finally, the eluate was collected, vacuum-freeze-dried, and desalted according to the C18 Zip Tips (Millipore) instructions for LC-MS/MS analysis.

LC-MS/MS analysis

The peptides were dissolved in liquid chromatography fluid phase A (0.1% formic acid and 2% acetonitrile) and separated using a NanoElute ultra-high-performance liquid chromatography system (Bruker Daltonics). Subsequently, in fluid phase B containing 0.1% formic acid and 100% acetonitrile solution, the peptides were separated in a gradient from 6% to 22% in 42 min, 22%–30% in 12 min, and 22%–80% in 3 min at a constant flow rate of 450 nL/min and held at 80% for the last 3 min.

The peptides were injected into a capillary ion source for ionization and analyzed using a TimsTOF Pro mass spectrometer. The ion source voltage was set at 1.5 kV. Both the peptide parent ion and its secondary fragments were analyzed using a TOF detector with a secondary mass spectrometry scan range of 100 to 1,700 m/z. The parallel-accumulated serial fragmentation mode was used for data acquisition. Each cycle involved ten parallel-accumulated serial fragmentation primary mass spectra acquisitions and secondary mass spectra with parent ion charges within the 0–5 range were selected. The dynamic exclusion time was set at 24 s to avoid repeated scans of the parent ions.

The targeting PRM analysis

Total protein extraction, trypsin digestion, and peptide enrichment were performed as described previously. The peptides were separated using an EASY-nLC 1200 ultra-high-performance liquid chromatography system after being dissolved in liquid chromatography fluid phase A. Liquid phase B was an aqueous solution containing 0.1% formic acid and 90% acetonitrile. The liquid phase gradient was set: 0–36 min, 9–25%; 36–54 min, 25–35%; 54–57 min, 35–80%; and 57–60 min, 80%, with the flow rate maintained at 500 nL/min. The peptides were injected into an ion source for ionization and analyzed using a Q Exactive HF-X mass spectrometer. The ion source voltage was set to 2.1 kV, and both the peptide parent ion and its secondary fragments were detected and analyzed using an Orbitrap. Using the PRM mode, the primary mass spectrometer was scanned over the 500–1,050 m/z range with a scanning resolution of 1,200,000. The resolution of the secondary MS scan was set at 15,000. A data-independent scan was used for the data acquisition mode, and the HCD collision energy was set at 28%. The automatic gain controls for the MS were set at 3E6 and 1E5. The maximum injection times for the ions were set at 50 ms and 220 ms, and the separation window was set at 1.4 m/z.

The MS results were analyzed using Skyline (v.21.1). Trypsin [KR/P] was chosen as the proteinase, the number of maximum missed cut sites was selected as four, and the peptide length was selected as 7–25 amino acid residues. Cysteine alkylation was set as a fixed modification, and lysine lactylation was set as a variable modification. The precursor ion charges were selected as two and three, the ion charge was one, and the ion types were b and y. The fragment ions were selected from the third to the last, and the mass error tolerance for ion matching was set at 0.02 Da.

Bioinformatics analysis

Raw data were processed using MaxQuant and the integrated Andromeda search engine (v.1.5.2.8), as described by Meng et al.[41] The subcellular localization of DLPs was predicted using Wolf Psort (v.3.0) software. Motif-x software was used to analyze sequence models consisting of 10 amino acids upstream and downstream of the Kla site for all protein sequences. GO functional annotation was performed using the EggNOG database. The KEGG database was used to annotate protein pathways. GO and KEGG enrichment significance analysis of DLPs was performed using Fisher's exact test (with identified proteins as background), and a p-value <0.05 was considered significant. The STRING database (v.11.5) was used to construct the PPI network, and Cytoscape (v.3.9.1) software was used to visualize the network.

QUANTIFICATION AND STATISTICAL ANALYSIS

Quantitative data are expressed as mean ± standard deviation. The differences between groups were assessed using an independent two-sample t-test, with $p < 0.05$ being statistically significant, and $p < 0.01$ being highly significant. Statistical analyses were performed using IBM SPSS Statistics for Windows, version 25.0. GraphPad Prism 8 software was used to draw bar, box, and pie plots.